DAXX represents a new type of protein-folding enabler

https://doi.org/10.1038/s41586-021-03824-5

Received: 21 December 2019

Accepted: 15 July 2021

Published online: 18 August 2021

Check for updates

Liangqian Huang[1,2], Trisha Agrawal[1,2,5], Guixin Zhu[1,2], Sixiang Yu[1,2], Liming Tao[3], JiaBei Lin[4], Ronen Marmorstein[2,4], James Shorter[4] & Xiaolu Yang[1,2]✉

Protein quality control systems are crucial for cellular function and organismal health. At present, most known protein quality control systems are multicomponent machineries that operate via ATP-regulated interactions with non-native proteins to prevent aggregation and promote folding[1], and few systems that can broadly enable protein folding by a different mechanism have been identified. Moreover, proteins that contain the extensively charged poly-Asp/Glu (polyD/E) region are common in eukaryotic proteomes[2], but their biochemical activities remain undefined. Here we show that DAXX, a polyD/E protein that has been implicated in diverse cellular processes[3–10], possesses several protein-folding activities. DAXX prevents aggregation, solubilizes pre-existing aggregates and unfolds misfolded species of model substrates and neurodegeneration-associated proteins. Notably, DAXX effectively prevents and reverses aggregation of its in vivo-validated client proteins, the tumour suppressor p53 and its principal antagonist MDM2. DAXX can also restore native conformation and function to tumour-associated, aggregation-prone p53 mutants, reducing their oncogenic properties. These DAXX activities are ATP-independent and instead rely on the polyD/E region. Other polyD/E proteins, including ANP32A and SET, can also function as stand-alone, ATP-independent molecular chaperones, disaggregases and unfoldases. Thus, polyD/E proteins probably constitute a multifunctional protein quality control system that operates via a distinctive mechanism.

DAXX was initially identified as an adaptor protein associated with the intracellular death domain of the apoptosis receptor Fas (also known as CD95 or Apo-1)[3,4]. It was subsequently implicated in additional apoptotic scenarios and a wide range of other cellular processes[5–10]. Deficiency of *Daxx* results in embryonic lethality in mice[11], whereas recurrent somatic mutations in *DAXX* are associated with human tumours[12,13]. Although in most cases a specific mechanism has been proposed for its action, the association of DAXX with numerous cellular proteins raises an intriguing question as to whether DAXX possesses a biochemical activity that underlies, or contributes to, its remarkably diverse functions. We reasoned that if such a unifying activity exists for DAXX, it might be related to protein folding. Here, we explore this possibility.

DAXX is an effective molecular chaperone

Molecular chaperones inhibit protein misfolding and aggregation[1]. To investigate whether DAXX can act as a molecular chaperone, we purified recombinant full-length DAXX protein from bacterial, insect and mammalian cells (Extended Data Fig. 1a–e) and tested it on the model chaperone substrate luciferase and neurodegeneration-associated, misfolding-prone proteins. When luciferase was incubated at an increased temperature, it lost enzymatic activity rapidly and coalesced into aggregates detectable by light scattering. DAXX purified from bacteria protected luciferase from heat-induced inactivation (Fig. 1a, Extended Data Fig. 1f) and aggregation (Fig. 1b), akin to HSP70 together with its co-chaperone HSP40. DAXX protein purified from insect Sf9 or human HEK293T cells also protected luciferase against thermal denaturation (Extended Data Fig. 1g–j).

Neurodegenerative disease-associated proteins can spontaneously assemble into aggregated species including amyloid fibrils[14]. When incubated in vitro, ataxin-1 protein with an expanded polyglutamine tract (ATXN1(82Q)), which is associated with spinocerebellar ataxia type 1, formed pelletable aggregates that were soluble with SDS. DAXX strongly prevented the aggregation of ATXN1(82Q), keeping almost all ATXN1(82Q) molecules in the supernatant (Fig. 1c).

Highly-ordered amyloid fibrils, which consist of β-strands that are stacked perpendicularly to the fibril axis (cross-β structure), are a pathological hallmark of neurodegenerative diseases including Parkinson's disease and Alzheimer's disease[14]. DAXX inhibited fibrillization of Parkinson's disease-associated protein α-synuclein (α-Syn), as shown by thioflavin T (ThT)-binding assay (Fig. 1d), electron microscopy (Fig. 1e) and a dot blot assay that detected SDS-resistant as well as SDS-soluble pelletable aggregates (Fig. 1f). A small amount of DAXX (0.1–0.4 μM)

[1]Department of Cancer Biology, Perelman School of Medicine, University of Pennsylvania, Philadelphia, PA, USA. [2]Abramson Family Cancer Research Institute, Perelman School of Medicine, University of Pennsylvania, Philadelphia, PA, USA. [3]Broad Institute of MIT and Harvard, Cambridge, MA, USA. [4]Department of Biochemistry and Biophysics, Perelman School of Medicine, University of Pennsylvania, Philadelphia, PA, USA. [5]Present address: Wilson Sonsini Goodrich & Rosati LP, New York, NY, USA. ✉e-mail: xyang@pennmedicine.upenn.edu

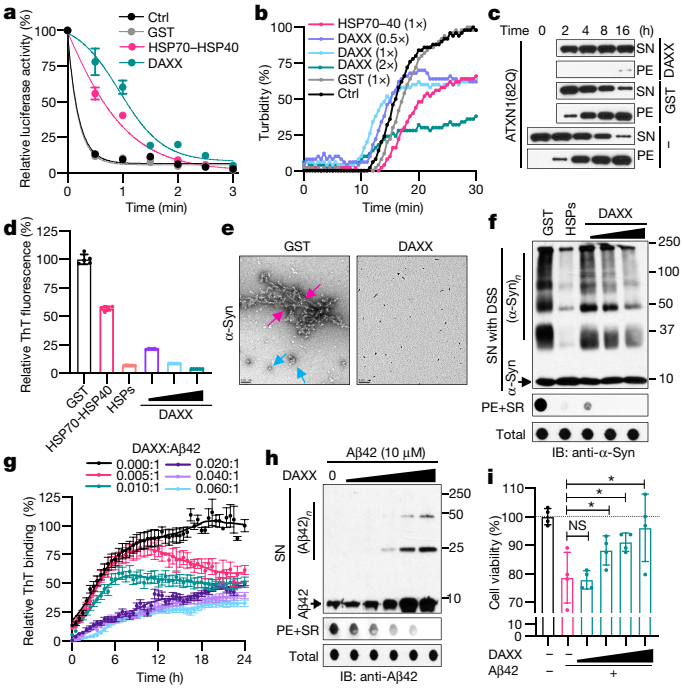

Fig. 1 | DAXX prevents protein misfolding and aggregation. **a**, **b**, Heat-induced luciferase inactivation (**a**, 5 nM) and aggregation (**b**, 200 nM) in presence or absence of GST, DAXX and HSP70–HSP40 at 200 nM (**a**) or at the indicated molar ratios (**b**). **c**, Aggregation of ATXN1(82Q) (50 nM) in the presence or absence of glutathione *S*-transferase (GST) or DAXX (200 nM each). Raw data for this and other gels are found in Supplementary Fig 1. PE, pelletable aggregates that were soluble with SDS; SN, supernatant. **d**–**f**, Fibrillization of α-Syn (70 μM) in the presence GST, HSP70–HSP40, HSPs (HSP70–HSP40–HSP104(A503S)) (200 nM each) and DAXX (100–400 nM) was assayed by ThT-binding (**d**), electron microscopy (**e**; red arrows, fibrils; blue arrows, large oligomers; scale bar, 100 nm), and sedimentation followed by dot blot for SDS-soluble and SDS-resistant (SR) aggregates and total α-Syn and by disuccinimidyl suberate (DSS) cross-linking for soluble oligomers (**f**). IB, immunoblot. **g**–**i**, Fibrillization of Aβ42 monomers (10 μM) in the absence or presence of DAXX (50–600 nM) (**g**, **h**), and viability of SH-SY5Y cells treated with Aβ42 pre-incubated with or without DAXX (**i**). An ATP-regeneration system was included with heat-shock proteins but not DAXX (all subsequent experiments with heat-shock proteins, but not experiments with DAXX, also contained an ATP-regeneration system). Data are mean or mean ± s.d. ($n = 4$ for **i**, and 3 for the rest) and are representative of three independent experiments. *$P < 0.05$, NS, not significant; unpaired Student's *t*-test.

was sufficient to prevent aggregation of α-Syn monomers that were approximately 175- to 700-fold in molar excess (70 μM). This activity of DAXX seemed to be stronger than that of HSP70–HSP40 and on a par with that of HSP70–HSP40 plus HSP104(A503S), a potentiated version of the yeast disaggregase HSP104 (ref. [15]).

Amyloid fibrils can propagate in a prion-like, self-templating manner, a property that probably underlies the spread of fibrillar aggregates along interconnected neuronal regions in patients[16]. Aggregation of soluble α-Syn monomers was accelerated by preformed fibrils (PFFs) of α-Syn (Extended Data Fig. 2a). DAXX suppressed this seeded fibrillization at sub-stoichiometric molar ratios to α-Syn monomers in a dose-dependent manner and near-completely blocked it at a relatively high dose (Extended Data Fig. 2b).

To further assess the effect of DAXX on protein fibrillization, we used a substrate with a stronger propensity to aggregate, the Alzheimer's disease-associated amyloid-β peptide Aβ42. DAXX inhibited fibrillization of Aβ42 at low molar ratios (1:200 to 1:17), maintaining it in a soluble state even after a prolonged incubation (Fig. 1g, h, Extended Data Fig. 2c–e). Consequently, in the presence of DAXX, Aβ42 monomers could not form PFFs that accelerated aggregation of fresh Aβ42 monomers (Extended Data Fig. 2f). Moreover, DAXX near-completely abolished Aβ42 PFF-induced aggregation of fresh Aβ42 monomers (Extended Data Fig. 2g). Therefore, DAXX suppresses both spontaneous and seeded aggregation of disease-associated proteins.

Preceding fibrillization, α-Syn and Aβ42 monomers form soluble oligomers that are neurotoxic[17]. DAXX blocked the formation of α-Syn oligomers of various sizes, akin to HSP70–HSP40–HSP104(A503S) (Fig. 1e, f). Moreover, although Aβ42 peptides pre-incubated alone were toxic to human neuroblastoma SH-SY5Y cells, Aβ42 peptides pre-incubated with DAXX displayed minimal toxicity (Fig. 1i). Therefore, DAXX prevents the formation of toxic prefibrillar oligomers.

Unlike canonical chaperones, the activity of DAXX did not require the addition of ATP (Fig. 1, Extended Data Figs. 1f–j, 2b–h); nor was it affected by the treatment of the ATP-diphosphohydrolase apyrase (Extended Data Fig. 2h, i). DAXX was unable to bind to ATP (Extended Data Fig. 2j). Canonical molecular chaperones often assemble into a dimer or a large oligomeric complex[1]. By contrast, size-exclusion chromatography and chemical crosslinking assay suggested that DAXX exists predominantly as a monomer (Extended Data Fig. 2k, l).

DAXX is a protein disaggregase

Disaggregases dissolve pre-existing protein aggregates, permitting refolding of misfolded proteins and hence avoiding the energetically costly process of protein degradation and re-synthesis[18]. DAXX protein purified from bacteria was able to dissolve luciferase aggregates generated by thermal denaturation and reactivate them in a time- and dose-dependent manner (Fig. 2a, Extended Data Fig. 3a–c). DAXX protein purified from Sf9 or HEK293T cells exhibited a similar ability (Extended Data Fig. 3d–f). DAXX achieved a maximal recovery of luciferase activity at fivefold excess (Extended Data Fig. 3g). A circular dichroism spectroscopic analysis showed DAXX reduced the β-strand content of heat-treated luciferase to a level close to that of unheated luciferase (Fig. 2b, Extended Data Fig. 3h), which indicates that DAXX returns the core structure of denatured luciferase to a nearly native state.

Although luciferase formed aggregates of relatively small sizes after heat treatment, it generated aggregates of large sizes upon urea treatment[19] (Extended Data Fig. 3i). DAXX exhibited little activity towards urea-produced luciferase aggregates, whereas HSP70–HSP40–HSP104(A503S) showed a modest activity (Extended Data Fig. 3j–l). When tested on disease-associated proteins, DAXX exhibited potent activity towards some, but not other, aggregates. DAXX readily disassembled the amorphous ATXN1(82Q) aggregates (Fig. 2c), and could also convert virtually all Aβ42 fibrils into a soluble state (Fig. 2d, e). However, DAXX was unable to dissolve α-Syn fibrils by itself; nor did it synergize with HSP70–HSP40–HSP104(A503S) for disaggregation (Extended Data Fig. 3m–p). As for its chaperone activity, the disaggregase activity of DAXX was independent of ATP (Fig. 2a–e, Extended Data Fig. 3).

DAXX is a protein unfoldase

Unfoldases can release stable misfolded monomers from kinetically trapped states, a property previously shown for the HSP70 chaperone system[15,20]. To test whether DAXX possesses unfoldase activity, we used the luciferase mutant LucDHis$_6$ (LucD), which adapts a compact, monomeric misfolded state upon repeated freeze–thaw cycles[20]. Misfolded LucD monomers bind more ThT than native LucD, reflecting a high β-sheet content[20]. DAXX decreased the binding of misfolded LucD monomers to ThT, consistent with unfoldase activity (Fig. 2f). Sensitivity to brief trypsin digestion is another indicator for the unfolded state[20] (Extended Data Fig. 4a). Incubation with DAXX for a short period of time (2 min) enhanced the sensitivity of LucD to trypsin, which

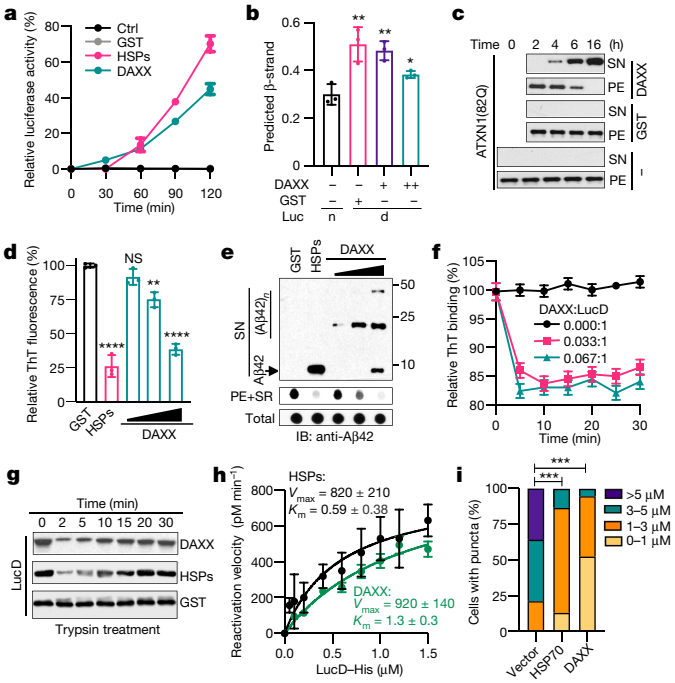

Fig. 2 | DAXX dissolves protein aggregates and unfolds misfolded species. **a**, Activity of heat-denatured luciferase (5 nM) treated with GST, DAXX or HSPs (100 nM each). **b**, β-stand contents of native luciferase or heat-denatured luciferase (1 μM each) treated with or without DAXX (0.1 and 0.5 μM). **c**, Sedimentation analysis of ATXN1(82Q) aggregates (50 nM) treated with or without of GST or DAXX (200 nM). **d**, **e**, ThT binding (**d**) and sedimentation (**e**) analyses of Aβ42 fibrils incubated with GST, HSPs (0.2 μM each) or DAXX (0.1, 0.2 and 0.4 μM). **f**, DAXX reduces the binding of monomeric misfolded LucD (3 μM) to ThT. **g**, Sensitivity to trypsin digestion of monomeric misfolded LucD (50 nM) after incubation with DAXX, GST or HSPs (100 nM each) for the indicated times. **h**, Kinetic analysis of LucD reactivation by DAXX or HSPs. **i**, Percentage of U2OS cells containing ATXN1(82Q) inclusions of different sizes in the presence or absence of DAXX or HSP70. Data are mean ± s.d. ($n = 3$) and are representative of two (**b**) or three (the rest) independent experiments. $^*P < 0.05$, $^{**}P < 0.01$, $^{***}P < 0.001$; unpaired Student's t-test for **b** and **d**, two-way analysis of variance (ANOVA) for **i**.

suggests rapid unfolding of the compact LucD monomers, whereas a longer incubation with DAXX (5–30 min) progressively reduced LucD sensitivity to trypsin while increasing its enzymatic activity (Fig. 2g, Extended Data Fig. 4b, c), which indicates the refolding of LucD to the native state. These effects of DAXX were similar to those of HSP70–HSP40–HSP104(A503S). Moreover, reactivation of LucD in the presence of DAXX followed saturation kinetics with maximum reaction rate (V_{max}) and Michaelis constant (K_m) values comparable to those in the presence of HSP70–HSP40–HSP104(A503S) (Fig. 2h). Collectively, these results suggest that DAXX serves as a catalyst to unfold misfolded monomers.

Effect of DAXX in cells

To evaluate the effect of DAXX on protein aggregation in cells, we co-expressed it with a nucleus-localized luciferase (nLuc) or its structurally destabilized derivative (nLucDM)[21] in HEK293T cells. DAXX increased the levels of nLucDM, but not nLuc, in a dose-dependent manner (Extended Data Fig. 4d). Moreover, in U2OS cells, DAXX reduced the size and number of ATXN1(82Q) inclusions, with an effect stronger than that of HSP70 (Fig. 2i, Extended Data Fig. 4e, f).

To further assess the effect of DAXX on oligomeric intermediates, we used a bimolecular fluorescence complementation (BiFC) system in which α-Syn was fused to the N-terminal (V1) or the C-terminal (V2) fragment of the Venus protein[22] (Extended Data Fig. 4g). When V1-α-Syn (V1S) and α-Syn-V2 (SV2) were expressed together, but not individually, reconstitution of the Venus fluorescence occurred (Extended Data Fig. 4h–j), reflecting α-Syn oligomerization that brought the split Venus moieties into proximity. DAXX markedly reduced the BiFC signal, but not V1S and SV2 protein levels (Extended Data Fig. 4h–j). Together, these results indicate that DAXX suppresses the formation of aggregates and prefibrillar oligomers in cells.

Role of the polyD/E domain

The various activities of DAXX in assisting protein folding suggested an intrinsic ability to recognize misfolded conformations. Consistently, when DAXX and nLuc were co-expressed in HEK293T cells, their interaction was increased upon heat shock (Extended Data Fig. 5a). In vitro, DAXX preferentially bound to heat-denatured over native luciferase (Extended Data Fig. 5b), which indicates that DAXX can distinguish misfolded and native conformers of the same polypeptide.

Canonical molecular chaperones and disaggregases can recognize linear peptide segments of unfolded proteins that are enriched in hydrophobic amino acids[1]. To define the molecular basis by which DAXX recognizes misfolded proteins, we generated a cellulose-bound peptide library consisting of peptides derived from luciferase, four physiologically relevant client proteins (p53, MDM2, H3.3 and H4)[6–8], and DAXX itself. DAXX bound to a small subset of this library (Extended Data Fig. 5c), which indicates its ability to discern peptides with different amino acid compositions. An analysis of the relative occurrence of each amino acid residue in DAXX-interacting peptides versus that in all peptides of the library revealed that DAXX strongly favoured basic residues Arg and Lys and, to a less extent, hydrophobic residues Ile and Leu, while disfavouring acidic residues Asp and Glu; polar residues Cys, Asn and Ser; and the aromatic residue Trp (Fig. 3a). Therefore, DAXX probably recognizes misfolded proteins in part through electrostatic interactions.

To test this notion, we examined the activity of DAXX to recover denatured luciferase in the presence of increasingly higher salt concentrations (0–300 mM KCl). The activity of DAXX initially strengthened (0–25 mM), reached a maximum (25–150 mM), and then progressively declined (150–300 mM) (Fig. 3b). By contrast, the activity of HSP70–HSP40–HSP104(A503S) remained largely unchanged (Fig. 3b). The decrease in DAXX activity at high ionic strength is consistent with the involvement of electrostatic interactions. But the initial increase in, and the subsequent maintenance of, its activity distinguish DAXX from polyanions such as nucleic acids[23], which show a monotonical decrease in activity with increasing salt[23]. Thus, DAXX might use electrostatic interactions in a regulated manner.

Of note, DAXX contains a region of mainly Asp and Glu[3] (Extended Data Fig. 5d). We generated mutants lacking this polyD/E region (ΔD/E) or consisting mostly of it (D/E) (Extended Data Fig. 5e). DAXX(ΔD/E) did not protect luciferase from heat inactivation (Fig. 3c), solubilize luciferase aggregates (Fig. 3d) or unfold LucD monomers (Extended Data Fig. 5f–h); nor did DAXX(D/E). Thus, the polyD/E region of DAXX is necessary, albeit insufficient, for various protein-folding activities.

Activity of other polyD/E proteins

Proteins that contain an extended polyD/E region with one or more continuous sequences of Asp and Glu (acidic runs) were first reported no later than the 1970s[24], and were subsequently found in various eukaryotes[2]. To investigate whether other polyD/E proteins can facilitate protein folding, we analysed ANP32A and SET, both of which contain a polyD/E region at their C termini[25,26] (Extended Data Fig. 6a). Recombinant ANP32A and SET proteins protected luciferase against heat-induced aggregation (Fig. 3e, f) and partially prevented

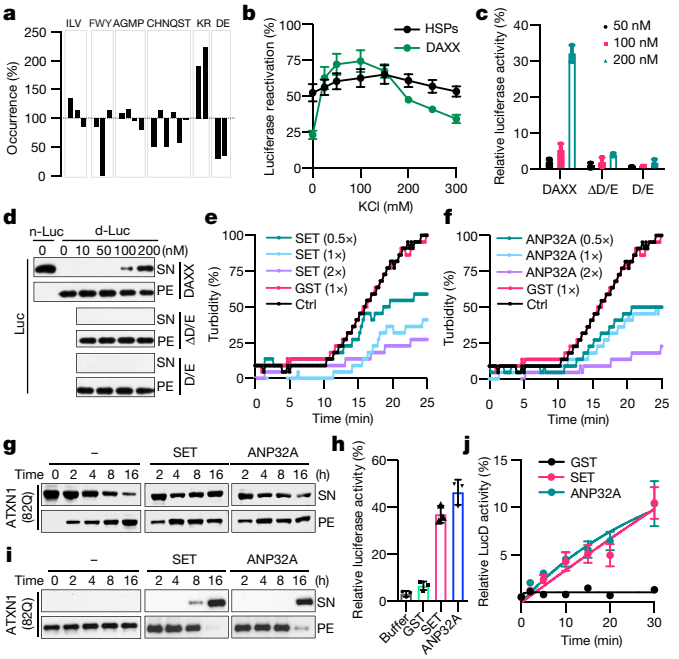

Fig. 3 | Other polyD/E proteins can function as molecular chaperones, disaggregases, and unfoldases. a, The occurrence of each amino acid in DAXX-binding peptides relative to its occurrence in the peptide library (100%). **b**, Reactivation of denatured luciferase (50 nM) by DAXX and HSPs (100 nM) in the presence of increasing salt concentration. **c**, **d**, Activity (**c**) and solubility (**d**) of denatured luciferase (d-Luc; 5 nM) after incubation with DAXX, DAXX(ΔD/E), or DAXX(D/E). n-Luc, native luciferase. **e**, **f**, Heat-induced aggregation of luciferase (200 nM) in the absence or presence of GST, ANP32A (**e**) or SET (**f**). **g**, **i**, Prevention (**g**) and reversal (**i**) of ATXN1(82Q) (50 nM) aggregation by SET and ANP32A (200 nM each). **h**, **j**, Reactivation of heat-denatured luciferase (5 nM) (**h**) and misfolded LucD monomers (50 nM) (**j**) by SET and ANP32A (200 nM each). Data are mean or mean ± s.d. ($n = 3$) and are representative of three independent experiments.

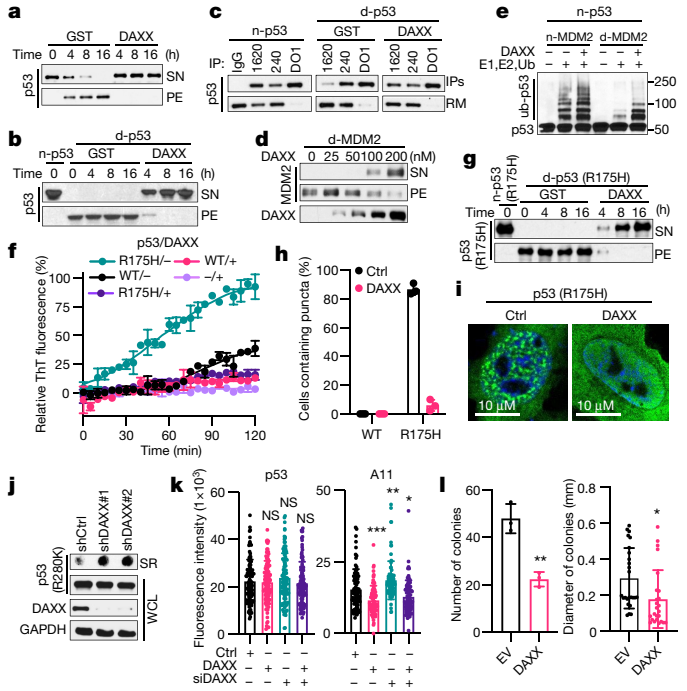

Fig. 4 | DAXX maintains and restores the native conformation of p53 and MDM2. a, Prevention of p53 (100 nM) aggregation by DAXX (200 nM). **b**, **d**, **g**, Solubilization of p53 (**b**), MDM2 (**d**) and p53(R175H) (**g**) (100 nM each) aggregates by DAXX (200 nM). **c**, Immunoprecipitation (IP) of native p53 (n-p53), or denatured p53 (d-p53) incubated with GST or DAXX, with PAb1620, PAb240 or DO1 (pan-p53 antibody). RM, proteins remained in supernatants. **e**, Ubiquitination of p53 (20 nM) by MDM2 (45 nM) in the presence or absence of DAXX (100 nM), or by denatured MDM2 (45 nM) pre-incubated with or without DAXX. **f**, Prevention of p53 and p53(R175H) (5 μM) fibrillization by DAXX (5 μM). **h**, **i**, Representative images of U2OS cells transfected with p53(R175H) or p53(R175H) plus DAXX (**h**), and percentage of cells containing p53(R175H) puncta (**i**). Scale bar, 10 μm. **j**, p53(R280K) aggregates in control and DAXX-knockdown MDA-MB-231 cells. **k**, Fluorescence intensity of anti-p53 (DO-1) and anti-pre-fibril oligomers (A11) staining in control MDA-MB-231 cells or MDA-MB-231 cells transfected with *DAXX* siRNAs and/or Flag–DAXX. **l**, Number and size of soft-agar colonies form by control and DAXX-overexpressing MDA-MB-231 cells. Data are mean ± s.d. and are representative of two (**j**) or three (the rest) independent experiments. *$P < 0.05$, **$P < 0.01$, ***$P < 0.001$; unpaired Student's *t*-test.

ATXN1(82Q) from spontaneous aggregation (Fig. 3g). Unlike DAXX, however, ANP32A and SET did not block α-Syn fibrillization (Extended Data Fig. 6b, c).

ANP32A and SET could also reactivate heat-denatured luciferase (Fig. 3h) and dissolve ATXN1(82Q) aggregates (Fig. 3i). Similar to DAXX, they were unable to reactivate urea-denatured luciferase (Extended Data Fig. 6d) or α-Syn fibrils (data not shown). ANP32A and SET could release misfolded LucD monomers from the energetically-trapped state and facilitate their re-folding (Fig. 3j, Extended Data Fig. 6e, f). Removing 14 amino acid or more from the SET polyD/E region markedly reduced its ability to reactivate luciferase (Extended Data Fig. 6g–i), which suggests that most of the polyD/E region is required for optimal activity.

PolyD/E proteins were previously surveyed on the basis of relatively long acidic runs[2,27]. An analysis of polyD/E domains in DAXX, ANP32A and SET showed that the occurrence of Asp and Glu residues is equal to, or greater than, 35 in a 50-amino acid window. Using this criterion, we searched various proteomes and identified a sizable number of polyD/E domain proteins in metazoans including 45 in humans and 51 in mice. These proteins also exist in *Arabidopsis* (25) and *S. cerevisiae* (18), but not in *E. coli*. (Extended Data Fig. 6j, Supplementary Table 1). Gene Ontology analysis showed that human polyD/E proteins are involved in various cellular processes (Extended Data Fig. 6k, l). The precise number of these proteins requires additional analysis of the composition of the polyD/E region that contributes to its activity. Nevertheless, polyD/E proteins seem to be prevalent in eukaryotic genomes, and their number has expanded significantly during evolution.

DAXX chaperones folding of p53 and MDM2

To evaluate whether polyD/E proteins promote the folding of their in vivo-validated client proteins, we examined the effect of DAXX on p53 and its ubiquitin ligase MDM2 (refs. [6,7]). p53 is a highly labile protein, and purified recombinant p53 readily misfolds and aggregates[28]. DAXX blocked p53 aggregation, keeping almost all p53 molecules in the soluble form (Fig. 4a). p53 can also form amyloid fibrils[29,30], which was also abrogated by DAXX (Extended Data Fig. 7a). Moreover, DAXX displayed potent disaggregase activity towards pre-existing p53 aggregates, converting virtually all of them back to the soluble state (Fig. 4b). By contrast, neither DAXX(ΔD/E) nor DAXX(D/E) exhibited chaperone and disaggregase activities towards p53 (Extended Data Fig. 7b, c).

Using antibodies specific to the wild-type (PAb1620) or mutant (PAb240) conformation of p53, we observed that DAXX restored misfolded p53 to its native conformation (Fig. 4c). Moreover, a thermal denaturation shift assay[31] showed that while DAXX did not significantly affect the transition temperature (T_m) of native p53, it increased the T_m of denatured p53 to that of native p53 (Extended Data Fig. 7d,e).

As for p53, DAXX was able to solubilize MDM2 molecules from aggregates and restored their native conformation (Fig. 4d, Extended Data

Fig. 7f–h). DAXX enhanced native MDM2-mediated ubiquitination of p53, and partially restored ligase activity to heat-treated MDM2 (Fig. 4e, Extended Data Fig. 7i). MDM2 ubiquitinated denatured p53 more readily than native p53. Pre-incubation with DAXX reduced ubiquitination of denatured p53 (Extended Data Fig. 7j), again indicating that DAXX restores the native conformation of p53.

Consistent with its ability to promote MDM2-mediated p53 ubiquitination, DAXX reduced p53 protein levels in U2OS cells (Extended Data Fig. 7k, l). DAXX also decreased p53 protein levels in H1299 cells where p53 was inducibly expressed, and lowered expression of p53 target genes (Extended Data Fig. 7m–o). Collectively, these results indicate that DAXX maintains the native conformation of both p53 and MDM2, enhancing the robustness of the p53-MDM2 regulatory network.

Effect of DAXX on mutant p53

p53 is the most frequently mutated gene in human tumours[32]. A substantial fraction of tumour-associated mutations destabilize conformation of p53 protein and accelerate its aggregation, contributing to more aggressive tumour phenotypes. To investigate whether DAXX can rescue the function of mutant p53, we used a 'hotspot' conformational mutation, R175H. Compared with wild-type p53, p53(R175H) aggregated at a faster pace. Still, DAXX nearly completely prevented p53(R175H) aggregation (Extended Data Fig. 8a). p53(R175H) more readily generated amyloid fibrils, which was again effectively blocked by DAXX (Fig. 4f). DAXX also rendered preformed p53(R175H) PFFs incapable of inducing fibrillization of wild-type p53 (Extended Data Fig. 8b). Furthermore, DAXX was able to transition nearly all pre-existing p53(R175H) insoluble aggregates back into solution (Fig. 4g). In U2OS cells, DAXX strongly reduced p53(R175H) aggregates that appeared as puncta (Fig. 4h, i, Extended Data Fig. 8c). DAXX also reduced protein, but not mRNA, levels of p53(R175H) in H1299 cells that inducibly express this mutant and increased the expression of p53 target genes including p21 and Puma (Extended Data Figs. 7m, n, 8d). These results suggest that DAXX converts p53(R175H) to the native state, rendering it responsive to MDM2-mediated degradation and restoring its normal function.

To further examine the influence of DAXX on mutant p53 and the associated oncogenic phenotypes, we chose breast cancer MDA-MB-231 cells, which contained the conformational mutant p53(R280K) that aggregates into amyloid fibrils[30]. Knocking down DAXX by independent small hairpin RNAs (shRNAs) increased intracellular p53(R280K) fibrillar aggregates (Fig. 4j, Extended Data Fig. 8e, f). Knocking down DAXX by a small interfering RNA (siRNA) yielded a similar result (Fig. 4k, Extended Data Fig. 8g). By contrast, forced expression of siRNA-resistant DAXX not only reversed the effect of the *DAXX* siRNA but also further decreased p53(R280K) aggregates (Fig. 4k, Extended Data Fig. 8g).

Knocking down DAXX increased proliferation of MDA-MB-231 cells on adherent plates (Extended Data Fig. 8h), and enhanced their ability to grow in soft-agar medium (Extended Data Fig. 8i, j), an in vitro measure of tumorigenicity. By contrast, forced expression of DAXX impeded adherent proliferation of MDA-MB-231 cells (Extended Data Fig. 8k) and reduced the number and size of soft-agar colonies formed by these cells by approximately 50% and 40%, respectively (Fig. 4l, Extended Data Fig. 8l). Collectively, these data suggest that DAXX may restore the native conformation and function to aggregation-prone p53 mutants, reducing their oncogenic properties.

Discussion

This study reveals that DAXX and other polyD/E proteins can participate in several aspects of protein quality control: preventing protein aggregation, dissolving preformed protein aggregates and unfolding monomeric misfolded proteins. The polyD/E proteins tested here seem to have different potencies, with DAXX being stronger than SET and ANP32A, which might reflect a hierarchy within this family or a difference in substrate specificity. DAXX is particularly effective for p53 and MDM2, which suggests that polyD/E proteins may be crucial for modulating conformation of their in vivo clients. Thus, DAXX and perhaps other polyD/E might have a role in both global and specific protein folding processes.

Protein folding and misfolding have been rationalized mainly in the context of hydrophobic interactions[1]. The involvement of the polyD/E region suggests that electrostatic interactions may also contribute substantially to protein folding and misfolding, as well as the mechanism of action of proteins containing this region. Nevertheless, DAXX does not merely act as a polyanion. Instead, the other portions of DAXX probably regulate the action of the polyD/E region in a dynamic manner. The importance of electrostatic interactions, along with ATP-independence and multifunctionality, indicate that polyD/E proteins may represent a new class of protein-folding enablers, which are mechanistically distinct from canonical ATP-dependent systems as well as ATP-independent systems such as that consisting of tripartite motif (TRIM) proteins[33,34].

Given the prevalence of p53 mutations in human tumours, restoring thermostability and normal function of p53 mutants would be highly beneficial for cancer therapy[35]. Nevertheless, development of small compounds to achieve such an outcome is challenging even for a single p53 mutant. This study suggests that DAXX can restore activity to a wide range of p53 mutants. Therefore, bolstering DAXX function might represent an alternative approach to therapeutically re-establish the tumour suppressive function of mutant p53.

Online content

Any methods, additional references, Nature Research reporting summaries, source data, extended data, supplementary information, acknowledgements, peer review information; details of author contributions and competing interests; and statements of data and code availability are available at https://doi.org/10.1038/s41586-021-03824-5.

1. Balchin, D., Hayer-Hartl, M. & Hartl, F. U. In vivo aspects of protein folding and quality control. *Science* **353**, aac4354 (2016).
2. Karlin, S., Brocchieri, L., Bergman, A., Mrazek, J. & Gentles, A. J. Amino acid runs in eukaryotic proteomes and disease associations. *Proc. Natl Acad. Sci. USA* **99**, 333–338 (2002).
3. Yang, X., Khosravi-Far, R., Chang, H. Y. & Baltimore, D. Daxx, a novel Fas-binding protein that activates JNK and apoptosis. *Cell* **89**, 1067–1076 (1997).
4. Chang, H. Y., Nishitoh, H., Yang, X., Ichijo, H. & Baltimore, D. Activation of apoptosis signal-regulating kinase 1 (ASK1) by the adapter protein Daxx. *Science* **281**, 1860–1863 (1998).
5. Perlman, R., Schiemann, W. P., Brooks, M. W., Lodish, H. F. & Weinberg, R. A. TGF-beta-induced apoptosis is mediated by the adapter protein Daxx that facilitates JNK activation. *Nat. Cell Biol.* **3**, 708–714 (2001).
6. Zhao, L. Y. et al. Negative regulation of p53 functions by Daxx and the involvement of MDM2. *J. Biol. Chem.* **279**, 50566–50579 (2004).
7. Tang, J. et al. Critical role for Daxx in regulating Mdm2. *Nat. Cell Biol.* **8**, 855–862 (2006).
8. Lewis, P. W., Elsaesser, S. J., Noh, K. M., Stadler, S. C. & Allis, C. D. Daxx is an H3.3-specific histone chaperone and cooperates with ATRX in replication-independent chromatin assembly at telomeres. *Proc. Natl Acad. Sci. USA* **107**, 14075–14080 (2010).
9. Song, M. S. et al. The deubiquitinylation and localization of PTEN are regulated by a HAUSP-PML network. *Nature* **455**, 813–817 (2008).
10. Mahmud, I. & Liao, D. DAXX in cancer: phenomena, processes, mechanisms and regulation. *Nucleic Acids Res.* **47**, 7734–7752 (2019).
11. Michaelson, J. S., Bader, D., Kuo, F., Kozak, C. & Leder, P. Loss of Daxx, a promiscuously interacting protein, results in extensive apoptosis in early mouse development. *Genes Dev.* **13**, 1918–1923 (1999).
12. Jiao, Y. et al. DAXX/ATRX, MEN1, and mTOR pathway genes are frequently altered in pancreatic neuroendocrine tumors. *Science* **331**, 1199–1203 (2011).
13. Gopal, R. K. et al. Widespread chromosomal losses and mitochondrial DNA alterations as genetic drivers in hurthle cell carcinoma. *Cancer Cell* **34**, 242–255 (2018).
14. Knowles, T. P., Vendruscolo, M. & Dobson, C. M. The amyloid state and its association with protein misfolding diseases. *Nat. Rev. Mol. Cell Biol.* **15**, 384–396 (2014).
15. Jackrel, M. E. et al. Potentiated Hsp104 variants antagonize diverse proteotoxic misfolding events. *Cell* **156**, 170–182 (2014).
16. Jucker, M. & Walker, L. C. Self-propagation of pathogenic protein aggregates in neurodegenerative diseases. *Nature* **501**, 45–51 (2013).
17. Kayed, R. et al. Common structure of soluble amyloid oligomers implies common mechanism of pathogenesis. *Science* **300**, 486–489 (2003).

18. Saibil, H. Chaperone machines for protein folding, unfolding and disaggregation. *Nat. Rev. Mol. Cell Biol.* **14**, 630–642 (2013).
19. Glover, J. R. & Lindquist, S. Hsp104, Hsp70, and Hsp40: a novel chaperone system that rescues previously aggregated proteins. *Cell* **94**, 73–82 (1998).
20. Sharma, S. K., De los Rios, P., Christen, P., Lustig, A. & Goloubinoff, P. The kinetic parameters and energy cost of the Hsp70 chaperone as a polypeptide unfoldase. *Nat. Chem. Biol.* **6**, 914–920 (2010).
21. Gupta, R. et al. Firefly luciferase mutants as sensors of proteome stress. *Nat. Methods* **8**, 879–884 (2011).
22. Outeiro, T. F. et al. Formation of toxic oligomeric alpha-synuclein species in living cells. *PLoS ONE* **3**, e1867 (2008).
23. Rentzeperis, D., Jonsson, T. & Sauer, R. T. Acceleration of the refolding of Arc repressor by nucleic acids and other polyanions. *Nat. Struct. Biol.* **6**, 569–573 (1999).
24. Walker, J. M., Hastings, J. R. & Johns, E. W. A novel continuous sequence of 41 aspartic and glutamic residues in a non-histone chromosomal protein. *Nature* **271**, 281–282 (1978).
25. Adachi, Y., Pavlakis, G. N. & Copeland, T. D. Identification and characterization of SET, a nuclear phosphoprotein encoded by the translocation break point in acute undifferentiated leukemia. *J. Biol. Chem.* **269**, 2258–2262 (1994).
26. Vaesen, M. et al. Purification and characterization of two putative HLA class II associated proteins: PHAPI and PHAPII. *Biol. Chem. Hoppe Seyler* **375**, 113–126 (1994).
27. Wang, D. et al. Acetylation-regulated interaction between p53 and SET reveals a widespread regulatory mode. *Nature* **538**, 118–122 (2016).
28. Butler, J. S. & Loh, S. N. Folding and misfolding mechanisms of the p53 DNA binding domain at physiological temperature. *Protein Sci.* **15**, 2457–2465 (2006).
29. Ishimaru, D. et al. Fibrillar aggregates of the tumor suppressor p53 core domain. *Biochemistry* **42**, 9022–9027 (2003).
30. Ano Bom, A. P. et al. Mutant p53 aggregates into prion-like amyloid oligomers and fibrils: implications for cancer. *J. Biol. Chem.* **287**, 28152–28162 (2012).
31. Zhang, R. & Monsma, F. Fluorescence-based thermal shift assays. *Curr. Opin. Drug Discov. Devel.* **13**, 389–402 (2010).
32. Muller, P. A. & Vousden, K. H. Mutant p53 in cancer: new functions and therapeutic opportunities. *Cancer Cell* **25**, 304–317 (2014).
33. Guo, L. et al. A cellular system that degrades misfolded proteins and protects against neurodegeneration. *Mol. Cell* **55**, 15–30 (2014).
34. Zhu, G. et al. TRIM11 prevents and reverses protein aggregation and rescues a mouse model of Parkinson's disease. *Cell Rep.* **33**, 108418 (2020).
35. Bykov, V. J. N., Eriksson, S. E., Bianchi, J. & Wiman, K. G. Targeting mutant p53 for efficient cancer therapy. *Nat. Rev. Cancer* **18**, 89–102 (2018).

Methods

Data reporting

No statistical methods were used to predetermine sample size. The experiments were not randomized and the investigators were not blinded to allocation during experiments and outcome assessment.

Antibodies and recombinant proteins

Antibodies against the following proteins/epitopes were purchased from the indicated sources: GAPDH (sc-47724), His tag (sc-8036), GST (sc-138), p53 (DO1, sc-126), MDM2 (sc-965), DAXX (sc-8043), α-synuclein (syn211, sc-12767) (Santa Cruz Biotechnology); Flag tag (14793) and DAXX (4533S) (Cell Signaling Technology); p53 (PAb1620, OP33; PAb240, OP29), MDM2 (OP46) (Calbiochem); HA tag (ab137838) and luciferase (ab21176) (Abcam); and β-Amyloid 1-42 (Aβ42, 805509) (BioLegend). HRP-conjugated anti-rabbit IgG (7074S) and anti-mouse IgG (7076S) antibodies were purchased from Cell Signaling Technology; IRDye 800CW (926-32211, anti-Rabbit) and IRDye 680RD (926-68070, anti-Mouse) secondary antibodies from Li-Cor; anti-Flag M2 Affinity Gel (A2220), 3xFlag peptide (F4799), firefly luciferase (L9420), and Aβ42 (A9810) from Sigma Aldrich; HSP70 (human HSP72, ADI-NSP-555), HSP40 (human HDJ1, ADI-SPP-400), and ATP regeneration solution (BML-EW9810-0100) from Enzo Life Sciences; and 6xHis-ubiquitin (U-530), UBE1 (E-304), and UBE2D2 (E2-622) from Boston Biochem. α-Synuclein (RP-003, RP-001) was purchased from Proteos. For western blot, anti-DAXX, p53, MDM2, and α-synuclein antibodies were used at 1:1,000 dilution, IRDye 800CW and IRDye 680RD at 1:10,000 dilution, and all other antibodies at 1:2,000 dilution.

Plasmids

Plasmids encoding HA–DAXX, Flag–DAXX, Flag–DAXX(ΔD/E), Flag–p53, Flag–p53(R175H), Flag–MDM2, Flag–ATXN1(82Q), HA–ATXN1(82Q), Flag–nFluc–GFP, and Flag–nFlucDM–GFP were constructed in pRK5, and GFP–HSP70 was constructed in pEGFP-C3, as previously described[7,33,34,36,37]. Plasmid expressing LucDHis$_6$, a *Photinus pyralis* luciferase variant in which the C-terminal 62 residues were replaced by SKLSYEQDGLHAGSPAALE followed by a 6xHis tag (pT7lucC-His), was a gift from P. Goloubinoff[20]. V1S and SV2 plasmids were generated by cloning α-synuclein into pBiFC-VN173 (Addgene, #22010) and pBiFC-VC155 (Addgene, 22011), respectively. DAXX shRNA plasmids were generated into pLKO.1 with oligo sequences as following: shDAXX#1, GCCTGATA CCTTCCCTGACTA; shDAXX#2, GCCACACAATGCGATCCAGAA. Bacterial expression plasmid encoding GST-DAXX-6xHis and GST–DAXX(D/E) were generated in pGEX-1ZT, a derivative of pGEX-1λT that contains additional cloning sites. Plasmids encoding ANP32A, SET, and SET deletion mutants were generated in pET28a. For protein expression in insect cells, DAXX–6xHis was cloned into pFastBac-GST.

Cell culture

HEK293T, H1299, U2OS, MDA-MB-231, SH-SY5Y and Sf9 cells were purchased from ATCC. HEK293T cells were cultured in DMEM medium, H1299 cells in RPMI-1640 medium, MDA-MB-231 cells in L15 medium, U2OS cells in McCoy's 5 medium and SH-SY5Y cells in DMEM/F12 (1:1) medium, each containing penicillin/streptomycin and 10% FBS. These cells were cultured at 37 °C in a humidified incubator with 5% CO_2. Sf9 cells were cultured in Sf-900 III medium containing antibiotic-antimycotic at 27 °C.

Protein purification

HSP104(A503S) was purified as previously described[15]. To express DAXX in bacteria and insect cells, pGEX-GST-DAXX-6xHis was transformed into Rosetta 2 (Novagen), and pFB-GST-DAXX-6xHis was transformed in Sf9 cells. Cells were lysed with Ni-NTA lysis buffer (50 mM NaH_2PO_4, 300 mM NaCl, 10 mM imidazole at pH 8.0, 1 mM PMSF, 2 mM DTT and 1 mg ml^{-1} lysozyme) followed by sonication. Lysates were incubated with glutathione beads (GE Healthcare, 17527901) at 4 °C for 4 h to overnight. Glutathione beads were washed sequentially with Ni-NTA lysis buffer containing additional 0, 0.25, 0.5, 1, 0.5, 0.25 and 0 M KCl, respectively, and twice with AcTEV buffer (50 mM Tris-HCl at pH 8.0 and 0.5 mM EDTA). The beads were then incubated at 25 °C for 2–3 h with AcTEV protease (Invitrogen, 12575015) in AcTEV buffer supplemented with 25 mM DTT. The supernatant was collected and incubated with Ni-NTA beads (Invitrogen, R90115) at 4 °C for 2–4 h. The Ni-NTA beads were washed with Ni-NTA wash buffer (50 mM NaH_2PO4, 10 mM NaCl and 10 mM imidazole at pH 7.0) and eluted with Ni-NTA elution buffer (50 mM NaH_2PO_4, 10 mM NaCl and 500 mM imidazole at pH 7.0) at 4 °C for 1 h. After elution, DAXX–6xHis was loaded onto PD 10 desalting columns (GE Health, GE17-0851) with Tris Buffer (20 mM Tris-HCl, 150 mM NaCl, pH 7.4, 2 mM DTT) or sodium phosphate buffer (20 mM sodium phosphate buffer pH 7.4, 0.2 mM EDTA, 0.02% sodium azide). 6xHis-tagged ANP32A, SET and SET fragments were purified from bacteria by Ni-NTA beads. GST and GST–DAXX(D/E) were purified from bacteria using glutathione beads and eluted with 35 mM reduced glutathione at 4 °C for 1 h.

To purify proteins from HEK293T cells, Flag–DAXX, Flag–p53, Flag–p53(R175H), Flag–MDM2 and Flag–ATXN1(82Q) were transfected into HEK293T cells. Cells were lysed in IP-lysis buffer (20 mM Tris-HCl at pH 7.4, 150 mM NaCl, 0.5% Triton X-100, 0.5% NP-40 and 10% glycerol) with sonication. Supernatants were incubated with anti-Flag M2 Affinity Gel (Sigma) at 4 °C for 4 h to overnight. The gel was washed sequentially with lysis buffers containing additional 0, 0.25, 0.5, 1, 0.5, 0.25 and 0 M KCl, and then with Tris buffer or sodium phosphate buffer. Recombinant proteins were eluted with 3×Flag peptide at 4 °C for 1 h.

Proteins was further purified by Mono Q (GE), Superdex 200 Increase 10/300 GL (GE), and/or Superose 6 10/300 GL columns that were driven by an NGC Chromatography System (Bio-Rad) or an AKTA FPLC system (GE Healthcare). DAXX–6xHis purified from bacteria was used in Figs. 1a, b, 2a, 3c; Flag–DAXX purified from HEK293T cells was used in Fig. 4a–g; and DAXX–6xHis purified from Sf9 cells was used in the other experiments unless otherwise indicated.

Prevention of protein misfolding and aggregation

For luciferase inactivation assay, 5 or 50 nM luciferase was heated at 42 °C alone or in the presence of the indicated proteins in luciferase refolding buffer (LRB: 25 mM HEPES-KOH at pH 7.4, 150 mM potassium acetate, 10 mM magnesium acetate and 10 mM DTT). Heat shock proteins were used as a positive control. ATP-Mg^{2+} and an ATP-regeneration system (Enzo Life Sciences) were included in samples with heat shock proteins, but not in samples with DAXX. When indicated, the concentration is referred to that of HSP70, and the concentrations of HSP40 and HSP104 were a half and twice, respectively, of that of HSP70. The concentration of HSP104 was that of monomers. Luciferase activities were measured using the Luciferase Assay System (Promega, E1500) in a Microplate Reader (BioTek). Data were acquired by BioTek Gen 5 and are expressed as percentages of the native luciferase control. To assay luciferase aggregation, 200 nM luciferase was heated at 42 °C alone or in the presence of indicated proteins in HEPES buffer (50 mM HEPES-KOH, pH7.4, 50 mM KCl, 5 mM $MgCl_2$ and 2 mM DTT). Luciferase aggregation was monitored by measuring the absorption at 600 nm in a Microplate Reader (BioTek).

Aggregation of ATXN1(82Q), p53, α-Syn and Aβ42 were assayed by sedimentation. After incubated in the presence of the indicated proteins at 37 °C with constant shaking, the reaction mixtures were centrifuged at 17,000*g* and 4 °C for 15–30 min. The supernatant fraction of α-Syn was treated with or without 0.1 mM disuccinimidyl suberate (DSS, Thermo Scientific, 21555) at 25 °C for 30 min. The pellet and supernatant fractions were then separated and analysed by western blot. For α-Syn and Aβ42, the SDS-soluble and SDS-resistant aggregates in the pellet fraction, as well as the total inputs, were also examined by dot blot on nitrocellulose membrane.

Protein fibrillization

Spontaneous and/or PFF-induced fibrillization of α-Syn, Aβ42 and p53 was analysed by real-time quaking induced conversion assay (RT-QuIC) as previously described with modifications[30,38,39]. PFFs were created by incubating α-Syn (1 mg ml^{-1}), Aβ42 (10 μM) and p53(R175H) (10 μM) at 37 °C with continuous shaking (1,000 rpm) for 7 days, 1 day and 2 h, respectively. PFFs were sonicated for 2 min before use. α-Syn PFFs (133 nM) were added to human α-Syn monomers (13.3 μM) in Tris-HCl buffer (20 mM Tris-HCl, pH 7.4, 150 mM NaCl) in the presence of 10 μM ThT. Fibrillization of Aβ42 (10 μM) was performed in the sodium phosphate buffer (20 mM sodium phosphate buffer, pH 8.0, 0.2 mM EDTA, 0.02% sodium azide) with 10 μM ThT. When indicated, Aβ42 PFFs (6 nM) was added to induce fibrillization. Fibrillization of p53 and p53(R175H) (5 μM) was performed in Tris-HCl buffer with 25 μM ThT. When indicated, p53(R175H) PFFs (1 μM) was used to induce fibrillization. RT-QuIC assay was performed in Nunc MicroWell 96-well optical-bottom plates in a microplate reader (BioTek). The reaction mixtures were incubated at 37 °C and shaken intermittently (1-min shake–1-min rest cycle) for the indicated durations. ThT fluorescence was recorded every 2, 5 or 15 min throughout the experiment.

Fibrillization of α-Syn was also assayed by transmission electron microscopy at the Electron Microscopy Resource Laboratory at the University of Pennsylvania. Samples were stained via negative staining and scanned by FEI Tecnai-12 electron microscope.

Disaggregation and reactivation of protein aggregates

Firefly luciferase (Sigma) was heat inactivated at 42 °C for 10 min and distributed to reactions at a final concentration of 5 or 50 nM in luciferase refolding buffer. Denatured luciferase incubated with indicate proteins at 25 °C for 90 min or the indicated times. Reaction mixtures were assayed for luciferase activity, as well as for luciferase solubility by sedimentation.

α-Syn fibrils (0.5 μM of monomer concentration) were incubated with GST (0.5 μM), DAXX–6xHis (0.25, 0.5 or 1 μM) or HSPs (0.5 μM) in the presence of an ATP regeneration system (Enzo) for 90 min at 30 °C. The samples were centrifuged at 17,000*g* and 4 °C for 20 min. The supernatants were removed, and the pellets were boiled in pellet buffer (50 mM Tris-HCl, pH 8.0, 8 M urea, 150 mM NaCl plus protease inhibitor cocktail). The total, supernatant, and pellet samples were then blotted on nitrocellulose membrane and incubated with anti-α-Syn antibody. Samples were quantified using ImageJ and normalized as (signal in supernatant)/(signal in pellet + signal in supernatant).

Aggregated ANTX1(82Q), p53 and p53(R175H) were generated by incubating these proteins at 37 °C shaking for 24–48 h. Aggregated MDM2 was generated by heat-inactivation at 50 °C for 10-15 min. Aggregated ATXN1(82Q), p53 and MDM2 proteins were centrifuged at 17,000*g* for 15 min. Pellets were resuspended and were incubated with the indicated proteins at 25 °C. Reaction mixtures were centrifuged at 17,000*g* and 4 °C for 15 min. The pellet and supernatant fractions were then resuspended in sample buffer and analysed by western blot.

Unfoldase assays for LucD

LucD was inactivated by freeze–thaw circles, and monomers were isolated as previously described[20]. For ThT assay, misfolded LucD monomers (3 μM) were incubated with in the presence of indicated concentration of DAXX and 60 μM ThT. The addition of ThT had no detectable effects on the activity of DAXX. ThT binding was measured by microplate reader (BioTek) with excitation/emission spectrum 450/485 nm as previously described[20]. For trypsin digestion assay, LucD (50 nM) was incubated alone or in the presence of indicated proteins at 25 °C for different times. The samples were then treated with trypsin (2.5 μM) at 22 °C for 3 min and analysed by western blot[20]. Steady-state kinetics analysis was performed by incubating 100 nM DAXX or HSPs with misfolded LucD monomers at increasing concentrations for 30 min. Luciferase activity was assayed. Kinetic curves were fit and kinetic parameters, V_{max} and K_m, were calculated by nonlinear regression using the Michaelis–Menten calculated by Graphpad Prism 8.

Circular dichroism spectrometer

Heat-denatured luciferase (1 μM) was incubated with and without GST and DAXX as indicated in sodium phosphate buffer for 3 h. Ellipticity was recorded between 260 and 200 nm in a quartz cuvette with 10 mm path length at 25 °C using an Aviv Circular Dichroism spectrometer. Native and heat-denatured luciferase (1 μM each) were loaded as positive and negative controls, respectively. Raw data was analysed by CAPITO (https://data.nmr.uni-jena.de/capito/index.php). The background signal from the buffer or the buffer including DAXX was subtracted.

ATP-binding assay

Binding to ATP was assayed using the ATP Affinity Test Kit (AK-102, Jena Bioscience), which contained agarose beads conjugated with ATP via the phosphate moiety (AP-ATP-agarose), the ribose moiety (EDA-ATP), or the adenine base at different positions (8AH-ATP) and (6AH-ATP agarose), and blank agarose beads without ATP conjugation. Beads (50 μl slurry) were equilibrated three times with wash buffer and then incubated with DAXX–6xHis or HSP70 (1 μg each) at 4 °C for 3 h with slight agitation. The beads were then washed three times with wash buffer, and the bound proteins were eluted with elution buffer. Input and bound proteins were analysed by western blot.

Peptide array

Cellulose-bound peptide array was made for 600 peptides representing 6 protein sequences (luciferase, p53, MDM2, H3.3, H4 and DAXX) by Biopolymers and Proteomics Core, Koch Institute, MIT. The sequence was synthesized as linear 13 amino acids in length with 10 amino acids overlapping. Recombined DAXX was used to probe the peptide assay, and peptides that could bind to DAXX were detected by anti-DAXX antibody. The array was scanned, and relative amino acid occurrence was determined. The occurrence of each amino acid in probed peptides relative to its occurrence in all peptides was determined.

Thermal shift assay

Thermal shift assays were performed as previously described[31]. Denatured p53 or MDM2 (1 μM each) was incubated with or without DAXX at 25 °C overnight, in a total volume of 9 μl. One microlitre of Sypro Orange (Invitrogen, diluted 1:300 before use) was added to each sample in a 384-well plate format. The fluorescence intensity was monitored at the rate of 1 °C per min using an Applied Biosystems 7500 RT–PCR machine. DAXX signal was subtracted from the incubated samples as the background.

In vitro ubiquitination

Pre-denatured Flag–p53 (20 nM) or pre-denatured Flag–MDM2 (45 nM) was incubated with Flag–DAXX (100 nM) at 25 °C for 3 h. For pre-denatured MDM2, 20 nM Zn^{2+} was added into the reaction mixtures to facilitate the folding of the Zn^{2+}-chelating RING domain. The in vitro reaction was performed using 100 nM E1, 1 μM E2 and 2 μg His-ubiquitin (His-Ub) in a final volume of 20 μl reaction buffer (40 mM Tris-HCl at pH 7.6, 2.5 mM ATP and 2 mM DTT) with indicated proteins. The reaction was carried out at 37 °C for 1.5 h and was stopped by adding SDS (final concentration 1%) and boiling for 5 min. p53 and its ubiquitination was detected by western blot.

Aβ42 neurotoxic assay

Cytotoxicity of Aβ42 oligomers was assessed in SH-SY5Y cells seeded in 96-well plates using the CCK8 assay[34]. Aβ42 monomers (10 μM) were incubated with DAXX-6xHis (from Sf9 cells, 0.05, 0.1, 0.2, 0.4, and 0.6 μM) with constant shaking (1,000 rpm) at 37 °C for 24 h to form oligomers. The preformed oligomers were suspended in the cell culture medium

for 1 h and added to SH-SY5Y cells for 24 h. Viable cells were counted by CCK8 (Dojindo, CK04).

Immunofluorescence and BiFC assay

Cells were plated on coverslips and transfected with the indicated siRNAs, shRNAs and/or cDNAs. Cells were fixed with 4% paraformaldehyde in PBS for 15 min at room temperature and permeabilized with PBS containing 0.25% Triton X-100 for 10 min. Cells were washed with PBS for three times and blocked with 1% BSA in PBST for 30 min at room temperature, and were then incubated with indicated primary antibodies at 4 °C overnight, followed by fluorescence-labelled secondary antibodies incubation at room temperature for 1 h. The coverslips were mounted to glass slides in medium containing 4′,6-diamidino-2-phenylindole (DAPI) (H-1200; Vector Laboratories). For BiFC assay, V1S and SV2 plasmids were co-transfected into HEK293T cells in a molar ratio 1:1. Immunofluorescence were performed 24 h after transfection. Fluorescence images were acquired by confocal microscope (Zeiss LSM 880 with software Zeiss Zen 2.3) and analysed by Fiji (Image J 1.52p).

Soft agar colony formation

Cells were seeded at a density of 7,500 cells per well for MDA-MB-231 cells in the top layer of 0.36% soft agar premixed with culture medium supplemented with 10% FBS in 6-well plates and incubated at 37 °C for 3 weeks. Colonies were stained with 0.05% crystal violet in 4% paraformaldehyde solution for imaging and quantification as described[40]. Images were analysed by Fiji (Image J 1.52p).

Geneontology analysis

Geneontology analysis was performed by Panther Classification System (http://pantherdb.org).

Analysis of polyD/E proteins

All the reference proteomes fastas analysed during the current study are downloaded from Uniprot database, including *Homo sapiens* [UP000005640], mouse [UP00000589], *Caenorhabditis elegans* [UP000001940], *Arabidopsis* [UP000006548], yeast [UP000002311] and *Escherichia coli* [UP000000625]. D/E enrichment region definition: sum of the occurrence of Asp and the occurrence of Glu equal or greater than 35 in any 50 amino acid window defines as a D/E enrichment region ($(D + E)/50 \geq 35/50$). Python notebook was used to implement a D/E enrichment region search function. In brief, all the reference protein sequences were examined amino acid by amino acid from start to end in any possible 50-amino acids window. Once a D/E enrichment region has been found in the protein sequence, its start position, end position, counts of D, counts of E, and unique name of that protein were documented as an item. Finally, all the items of D/E enrichments were output as an excel file per species and then different isoforms of the same protein were excluded manually.

Quantification and statistical analysis

Quantification of protein bands on western blots, number and size of colonies in soft-agar medium, and fluorescence signals in cells were performed by ImageJ. Statistical analysis was performed by GraphPrism 8. Individual data points were shown in plots and charts. Data are presented as mean ± s.d. An unpaired Student's *t*-test was used to evaluate the statistical significance in the mean value between two populations ($^{*}P < 0.05$, $^{**}P < 0.01$, $^{***}P < 0.001$).

Reporting summary

Further information on research design is available in the Nature Research Reporting Summary linked to this paper.

Data availability

All data supporting the findings of this study are provided within the manuscript and its Supplementary Information. Source data are provided with this paper.

Code availability

Source code and datasets for polyD/E protein analysis are available in GitHub: https://github.com/SunmoonTao/de-enrichemnt-analysis.

36. Chu, Y. & Yang, X. SUMO E3 ligase activity of TRIM proteins. *Oncogene* **30**, 1108–1116 (2011).
37. Chen, L. et al. Enhanced degradation of misfolded proteins promotes tumorigenesis. *Cell Rep.* **18**, 3143–3154 (2017).
38. Yen, C. F., Harischandra, D. S., Kanthasamy, A. & Sivasankar, S. Copper-induced structural conversion templates prion protein oligomerization and neurotoxicity. *Sci. Adv.* **2**, e1600014 (2016).
39. Månsson, C. et al. Interaction of the molecular chaperone DNAJB6 with growing amyloid-beta 42 (Aβ42) aggregates leads to sub-stoichiometric inhibition of amyloid formation. *J. Biol. Chem.* **289**, 31066–31076 (2014).
40. Zhang, Y. et al. Upregulation of antioxidant capacity and nucleotide precursor availability suffices for oncogenic transformation. *Cell Metab.* **33**, 94–109 (2021).

Acknowledgements We thank S. K. Sharma and P. Goloubinoff for providing the LucD plasmid, D. Brady for help with protein purification, D. Ricketts and A. Olia for help with the thermal shift assay, J. Huang for technical assistance, and E. Dean for Sf9 protein production. This work was supported by National Institutes of Health (NIH) grants R01CA182675, R01CA184867, R01CA235760, R01CA243520 (X.Y.), P01 AG031862 (R.M.) and R01GM099836 (J.S.); an Alzheimer's Association Research Fellowship and a Warren Alpert Foundation Distinguished Scholars Fellowship (J.L.); and a Sponsored Research Agreement from Wealth Strategy Holding Limited (X.Y.).

Author contributions X.Y. conceived and supervised the study. L.H. and X.Y. designed the experiments. L.H. performed most experiments. T.A. initiated the study and performed part of in vitro assays. G.Z. helped with in vitro assays. S.Y. helped with p53-related experiments. L.T. performed protein sequence analysis. R.M. helped with protein production in insect cells and advised on thermal shift assay. J.S. and J.L. provided HSP104 protein and advised on protein folding assays. X.Y. and L.H. prepared the manuscript with major inputs from J.S. and R.M. and comments from all other authors.

Competing interests X.Y. is a founder and equity holder of Evergreen Therapeutics LLC, which received investments from Wealth Strategy Holding Limited. J.S. is a consultant for Dewpoint Therapeutics, Maze Therapeutics, Vivid Sciences, Korro Bio, and ADRx. The other authors declare no competing financial interests.

Additional information
Supplementary information The online version contains supplementary material available at https://doi.org/10.1038/s41586-021-03824-5.
Correspondence and requests for materials should be addressed to X.Y.
Peer review information *Nature* thanks Jerson Silva and the other, anonymous, reviewer(s) for their contribution to the peer review of this work. Peer review reports are available.
Reprints and permissions information is available at http://www.nature.com/reprints.

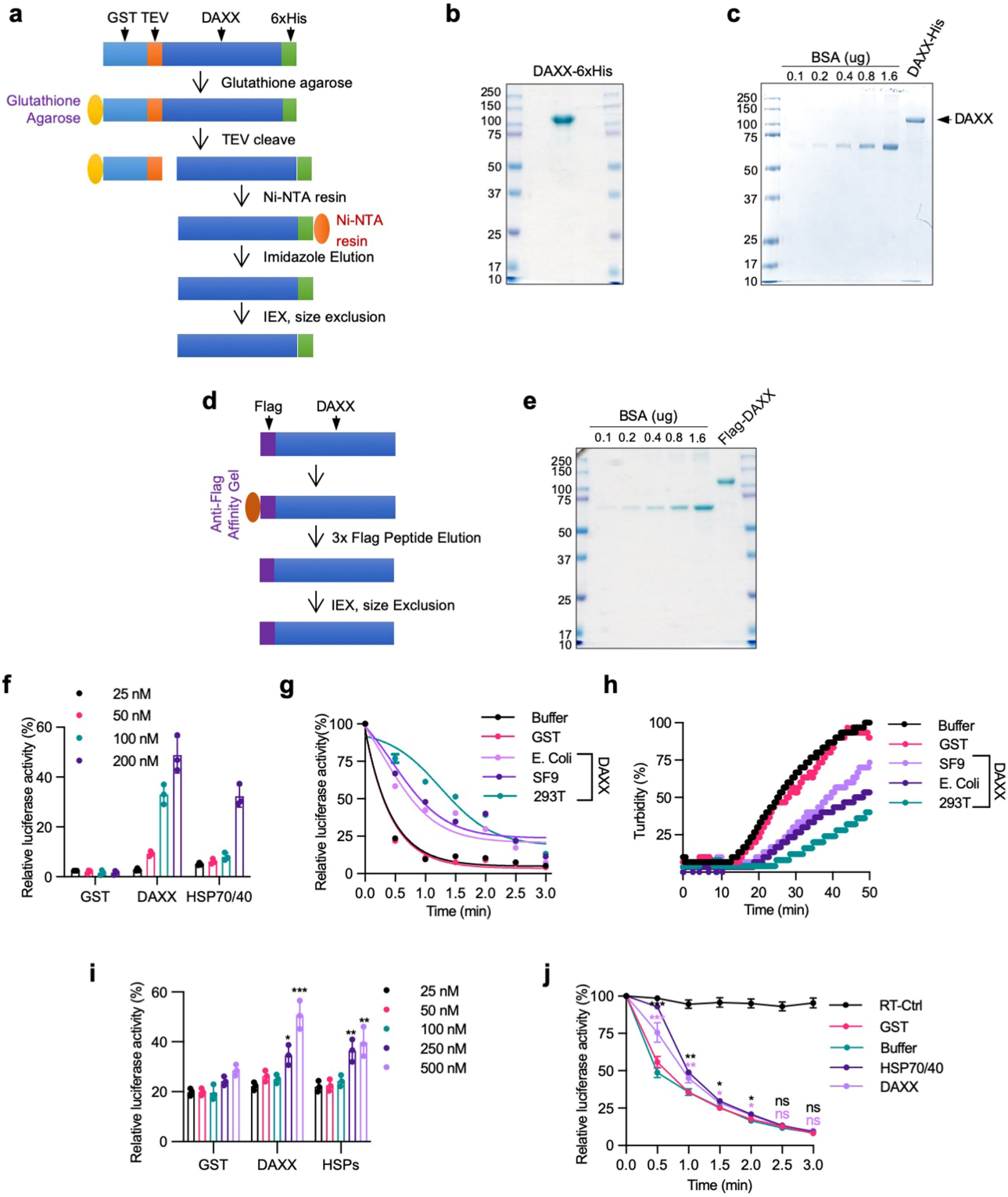

Extended Data Fig. 1 | See next page for caption.

Extended Data Fig. 1 | Purification of recombinant DAXX proteins and their ability to prevent luciferase misfolding and aggregation. a, Scheme for purifying DAXX–6xHis from bacteria BL21(DE3) and insect Sf9 cells. To generate full-length protein, DAXX was fused to GST at the N terminus with a TEV protease cleavage site inserted in between GST and DAXX, and to 6xHis at the C terminus. The fusion protein was first purified with glutathione resins. Beads-bound GST–DAXX–6xHis protein was treated with TEV protease to released DAXX–6xHis, which was subsequently purified with Ni-NTA resins. After elution with imidazole, DAXX-6xHis was further purified with ion-exchange and gel-filtration columns, and concentrated as needed. **b**, **c**, DAXX–6xHis purified from bacteria BL21(DE3) cells (**b**) and insect Sf9 cells (**c**) were analysed by SDS–PAGE and Coomassie blue staining. Bovine serum albumin (BSA) was used as a protein standard (**c**). Mass spectrometry analysis indicated that the vast majority of species in the minor bands of the DAXX preps were derived from DAXX. **d**, Scheme for purifying Flag–DAXX from HEK293T cells. Flag–DAXX was transiently transfected in HEK293T cells and purified using anti-Flag M2 beads. After elution with 3xFlag peptides, Flag–DAXX was further purified with ion-exchange and gel filtration columns, and concentrated as needed. **e**, Flag–DAXX purified from HEK293T cells was analysed by SDS–PAGE and Coomassie blue staining. Mass spectrometry analysis indicated that the vast majority of species in the minor bands of the DAXX preps were derived from DAXX. **f**–**h**, DAXX proteins purified from bacteria, insect cells, and mammalian cells protect luciferase from heat-induced inactivation and aggregation. Luciferase (**f**, **g**, 5 nM; **h**, 200 nM) was heated at 42 °C in the presence of indicated concentrations of GST, DAXX–6xHis (from bacteria) or HSP70 (plus HSP40 at a half concentration, same below) for 1 min (**f**), or in the presence or absence of GST, DAXX–6xHis (from bacteria), DAXX–6xHis (from insect cells), or Flag–DAXX (200 nM each) for the indicated times (**g**, **h**). Shown are luciferase activity relative to the native protein (**f**, **g**) and relatively turbidity measured at OD_{600} (**h**). The DAXX protein purified from HEK293T cells appeared to be more active than those purified from bacteria and insect cells **i**, **j**, Protective activity of DAXX for a higher amount of luciferase. Luciferase (50 nM) was heated at 42 °C in the presence of the indicated concentrations of GST, DAXX–6xHis (from Sf9 cells), or HSP70 for 1 min (**i**), or in the presence of absence of GST, DAXX–6xHis (Sf9 cells) or HSP70–HSP40 (200 nM each) for the indicated times. Luciferase activity was normalized to native protein. RT-CTRL, control luciferase sample kept at room temperature Assays in **b**, **c** and **e** have been performed three times with similar results. Numerical data are mean ± s.d. ($n = 3$) and are representative of three (**f**, **j**) or two (**g**, **h**, **i**) independent experiments. $^{*}P < 0.05$, $^{**}P < 0.01$, $^{***}P < 0.001$, ns, not significant; unpaired Student's *t*-test.

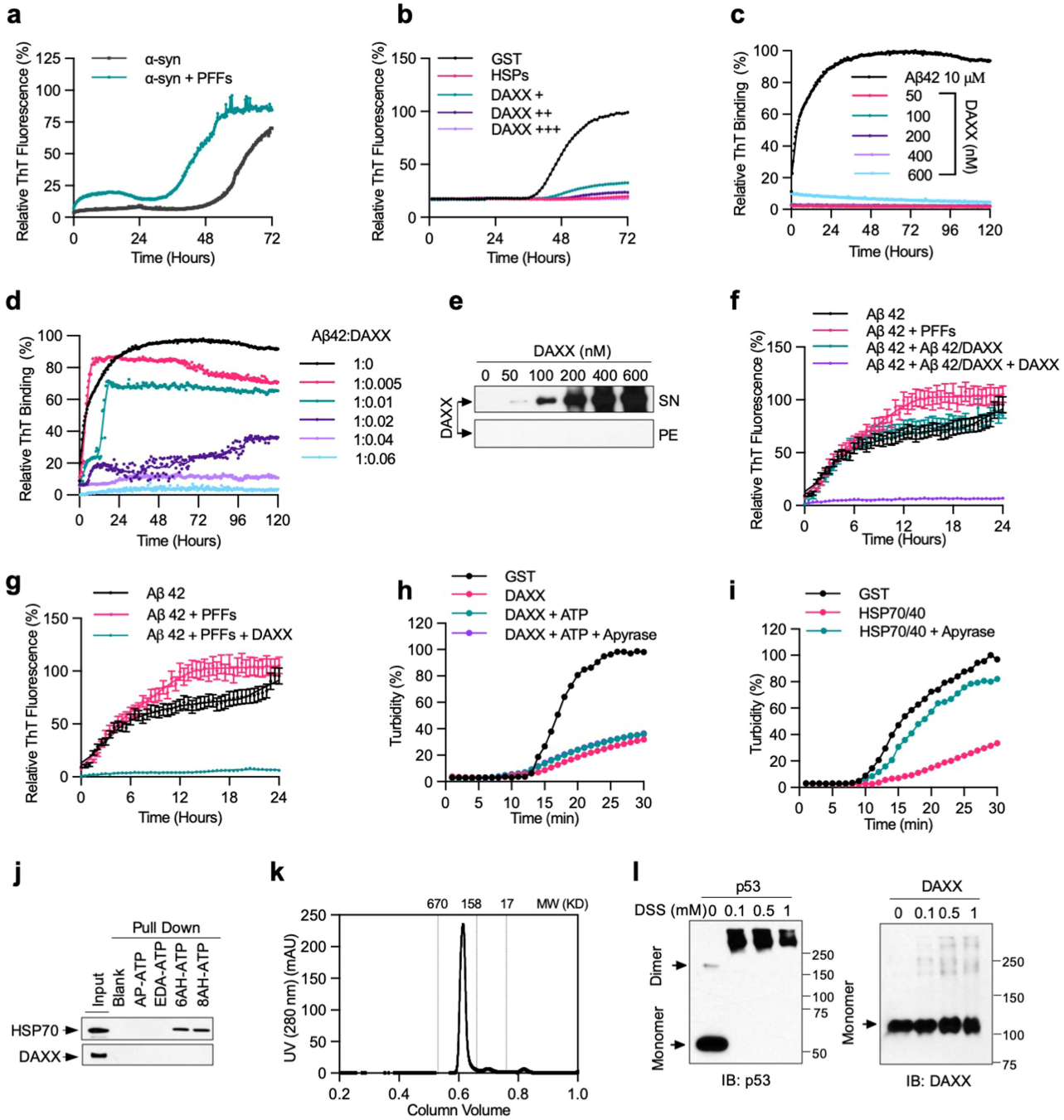

Extended Data Fig. 2 | See next page for caption.

Extended Data Fig. 2 | DAXX prevents α-Syn and Aβ42 aggregation, acts independently of ATP, and probably exists as a monomer. a, **b**, PFF-induced aggregation of soluble α-Syn monomers and its inhibition by DAXX. α-Syn monomers (13.3 μM) was incubated alone, together with in α-Syn PFFs (133 nM) (**a**), or together with in α-Syn PFFs (133 nM) in the presence of GST (0.2 μM), HSPs (0.2 μM HSP70, 0.1 μM HSP40, and 0.4 μM HSP104(A503S)), and DAXX–6xHis (from Sf9 cells, 0.1, 0.2,and 0.4 μM) (**b**). Aggregation was monitored by real-time quaking-induced conversion (RT-QuIC) assay. **c**–**e**, DAXX suppresses Aβ42 fibrillization for a prolonged incubation, during which DAXX itself did not form fibrils or other sedimentable aggregates. Aβ42 monomers (10 μM) and DAXX–6xHis (from Sf9 cells, 0.05, 0.1, 0.2, 0.4 and 0.6 μM) were incubated alone (**c**, **e**) or together (**d**) at 37 °C for 120 h. Formation of fibrils was analysed by ThT fluorescence assay (**c**, **d**). Solubility of DAXX was analysed by sedimentation assay (**e**). **f**, **g**, DAXX blocks Aβ42 monomers to form PFFs that accelerate aggregation of fresh Aβ42 monomers and Aβ42 PFF-induced aggregation of fresh Aβ42 monomers. Aβ42 monomers (10 μM) were incubated at 37 °C alone, together Aβ42 PFFs (6 nM) (**f**, **g**), Aβ42 (6 nM) preincubated with DAXX–6xHis (from Sf9 cells) at a 100:1 molar ratio (Aβ42/DAXX), Aβ42/DAXX plus DAXX–6xHis (0.6 μM) (DAXX) (**f**), or Aβ42 PFFs (6 nM) in the presence of DAXX (**g**). Formation of fibrils was analysed by ThT fluorescence assay. Assays in **f** and **g** were done at the same time. **h**, **i**, The chaperone activity of DAXX is not affected by the addition of ATP or the treatment of apyrase. Luciferase (0.2 μM) was heated at 42 °C in presence of GST (0.2 μM) (**h**, **i**), DAXX–6xHis (insect cells, 0.2 μM) with or without ATP (5 mM ATP-Mg^{2+} plus an ATP-regeneration system) and apyrase as indicated (**h**), or HSP70–HSP40 (0.2 and 0.1 μM, respectively) with or without apyrase (**i**). Aggregation formation was monitored by OD at 600 nm. **j**, DAXX does not bind to ATP. Recombinant DAXX–6xHis and HSP70 were incubated with agarose beads conjugated without ATP (–) or with ATP via the phosphate moiety (AP-ATP), ribose moiety (EDA-ATP), or the adenine base at different positions (6AH-ATP and 8AH-ATP). The input and pulldown samples were analysed by western blot. **k**, DAXX exists as a homogeneous species of relatively low molecular weights. Recombinant Flag–DAXX protein was analysed by Superdex 200 10/300 GL column. Proteins standards (in kDa) are indicated. **l**, DAXX likely exists as a monomer. Recombinant Flag–DAXX (1 μM) was crosslinked with indicated concentration of DSS at 25 °C for 30 min and analysed by western blot. Flag–p53 (1 μM), which is expected to be a tetramer, was used as control. Similar results were obtained for DAXX–6xHis. Assays have been performed three (**b**–**e**, **k**, **l**) or two (**a**, **h**, **i**, **j**) times with similar results. Numerical data are mean ± s.d. ($n = 3$) and are representative of three independent experiments (**f**, **g**).

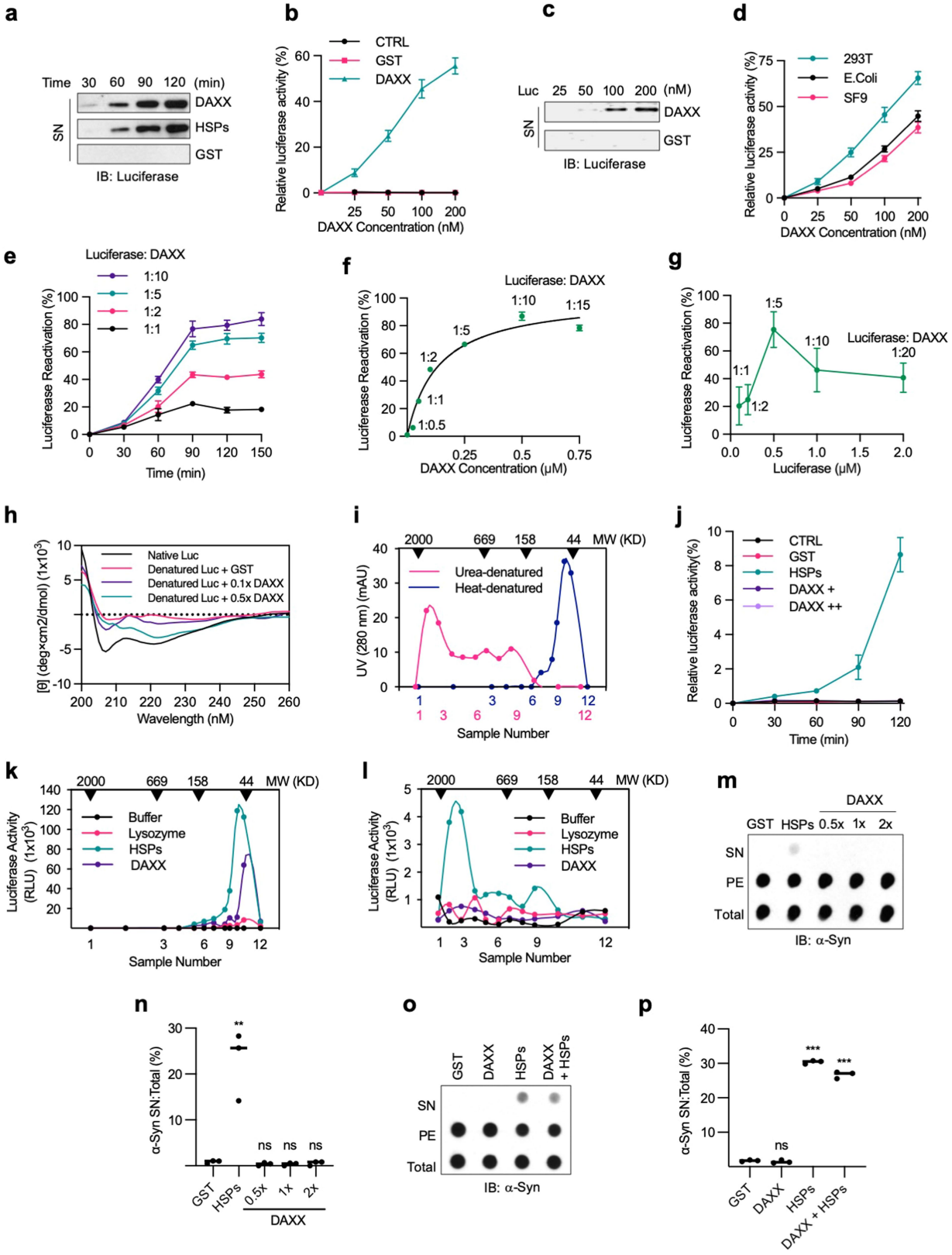

Extended Data Fig. 3 | See next page for caption.

Extended Data Fig. 3 | DAXX can dissolve small luciferase aggregates, but not large luciferase aggregates or α-Syn fibrils. a–**c**, DAXX dissolves and reactivates heat-denatured luciferase aggregates. Heat-denatured luciferase (5 nM) was incubated at 25 °C with GST (100 nM), DAXX–6xHis (from *E. coli*, 100 nM), and HSPs (100 nM HSP70, 50 nM HSP40 and 200 nM HSP104(A503S)) for the indicated times (**a**), or with the indicated amounts of GST or DAXX–6xHis for 90 min (**b**, **c**). Shown are luciferase activity relative to that of native luciferase (**b**), and the amount of luciferase in the SN after sedimentation (**a**, **c**). **d**, Disaggregase activity of DAXX proteins purified from different sources. Relative activity of heat-denatured luciferase (5 nM) that was incubated at 25 °C for 90 min with increasing concentrations of DAXX purified from the indicated sources. **e**, **f**, Disaggregase activity of DAXX for a higher amount of denatured luciferase. Relative activity of heat-denatured luciferase (50 nM) that was incubated at 25 °C with the increasing molar ratios of DAXX–6xHis (from Sf9 cells) for the indicated times (**e**) or 90 min (**f**). **g**, DAXX achieves the maximal recovery of luciferase activity at fivefold excess. Heat-denatured luciferase (0.1, 0.2, 0.5, 1 and 2 μM) was incubated with DAXX–6xHis (0.1 μM) at 25 °C for 90 min. Luciferase activity is relative to that of native luciferase. **h**, DAXX restores the native conformation to denatured luciferase. Native or heat-denatured luciferase (1 μM) incubated alone or together with GST (1 μM) or DAXX–6xHis (0.1×: 0.1 μM; 0.5×: 0.5 μM) for 90 min were examined by circular dichroism spectroscopy. Data were analysed by CAPITO, with the percentages of β-stand shown in Fig. 2b. **i**, Different sizes of luciferase aggregates generated by heat and urea treatments. Luciferase (1 μM) denatured by heat or urea was fractionated on Superdex 200 10/300 GL column. Fractions were analysed by western blot and the relative abundance of luciferase is indicated. **j**, DAXX cannot reactive urea-denatured luciferase. Relative activity of urea-denatured luciferase (5 nM) that was incubated with GST (0.2 μM), DAXX (0.2 and 1 μM), or HSPs (0.2 μM HSP70, 0.1 μM HSP40 and 0.4 μM HSP104(A503S)) at 25 °C for 90 min. **k**, **l**, Luciferase denatured by heat (**k**) or urea (**l**) was fractionated on gel filtration chromatography. Fractions in the range of 44 to 2,000 kDa were incubated with buffer, lysozyme (0.1 μM), DAXX–6xHis (0.1 μM), or HSP70–HSP40–HSP104(A503S) (0.1, 0.05 and 0.2 μM, respectively) at 25 °C for 90 min, and luciferase activity was determined. **m**–**p**, DAXX is unable to dissolve α-Syn fibrils. Preformed α-Syn fibrils (0.2 μM) were treated with GST (0.2 μM) (**m**–**p**), DAXX–6xHis at the indicated molar ratios (**m**, **n**) or at 0.2 μM (**o**, **p**), HSPs (0.2 μM HSP70, 0.1 μM HSP40, and 0.4 μM HSP104(A503S) plus ATP and an ATP regeneration system) (**m**–**p**), or both DAXX and HSPs (**o**, **p**). Reactions mixtures were analysed by dot blot (**m**, **o**), and soluble α-Syn relative to total α-Syn was quantified (**n**, **p**) ($n = 3$). Assays in **a**, **c**, **h**, **i**, **k**–**p** have been performed three times with similar results. Numerical data are mean ± s.d. ($n = 3$) and are representative of three independent experiments (**b**, **d**-**g**, **j**). $^{**}P < 0.01$, $^{***}P < 0.001$; unpaired Student's *t*-test.

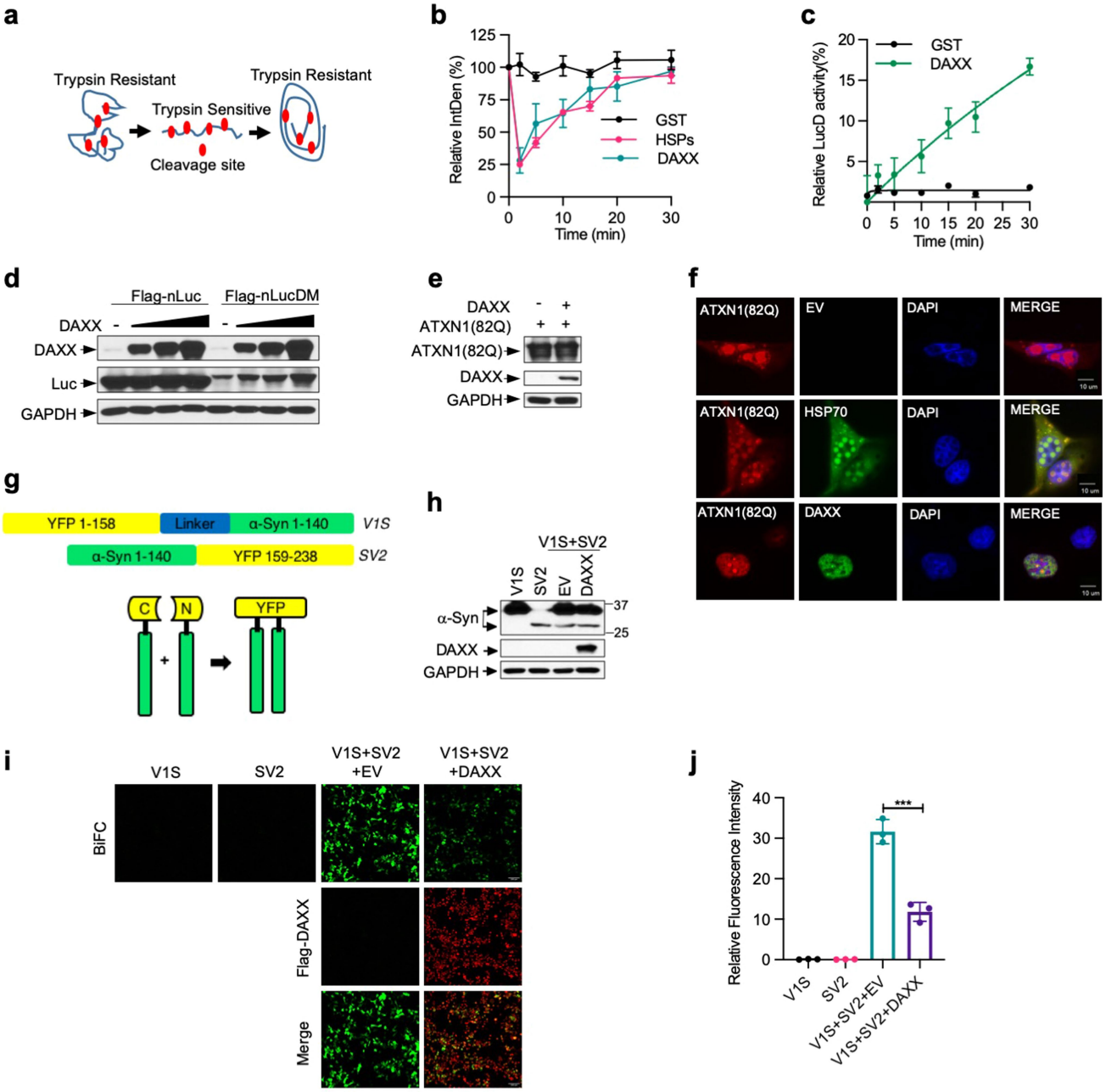

Extended Data Fig. 4 | DAXX unfolds misfolded LucD and protects against protein aggregation and oligomerization in cells. a, A schematic representation of compact misfolded LucD monomers, the unfolded intermediates, and the native conformers, as well as their sensitivity to brief trypsin digestion. **b**, DAXX changes trypsin sensitivity of LucD. LucD (50 nM) was incubated with DAXX-–xHis (100 nM), GST (100 nM), or HSPs (100 nM HSP70, 50 nM HSP40 and 200 nM HSP104(A503S)) at 25 °C. At indicated time points, aliquots of luciferase were incubated with 2.5 μM trypsin at 22 °C for 2 min and were analysed by western blot. Shown is luciferase band intensity. A representative western blot is presented in Fig. 2g. **c**, DAXX increases the enzymatic activity of LucD. Misfolded LucD monomers (50 nM) were incubated with GST (100 nM) or DAXX–6xHis (100 nM) for indicated durations and assayed for luciferase activity. **d**, DAXX elevates the levels of nLucDM, but not nLuc, in cells. nLuc or nLucDM was transfected together with empty vector (EV) or Flag–DAXX in HEK293T cells. Cell lysates were analysed by western blot 24 h after transfection. **e**, **f**, DAXX reduces aggregation, but not expression, of ATXN1(82Q) in cells. U2OS cells transfected with HA-Atxn1-82Q together with EV, Flag–DAXX (**e**, **f**) or GFP–HSP70 (**f**) were analysed by western blot (**e**), or immunofluorescence with anti-HA (red) and anti-Flag (green) antibodies (**f**; scale bar, 10 μm). Quantification of the percentage of cells containing different sizes Atxn1-82Q inclusions is shown in Fig. 2i. **g**, Schematic representation of BiFC assay based on Venus, an improved version of yellow fluorescent protein (YFP). **h**–**j**, DAXX inhibits α-Syn oligomerization in cells. HEK293T cells were transfected with V1S and SV2 individually, or together with empty vector (EV) or DAXX. Cells were analysed by western blot for protein expression (**h**) and by fluorescence microscopy for BiFC signals and Flag–DAXX expression (**i**; scale bars, 100 μm), with the quantification of BiFC signals shown in **j**. Assay in **d**, **e**, **f**, **h** and **i** have been performed two times with similar results. Numerical data are mean ± s.d. ($n = 3$) and are representative of three independent experiments (**b**, **c**, **j**). $^{*}P < 0.05$, $^{**}P < 0.01$, $^{***}P < 0.001$; unpaired Student's t-test.

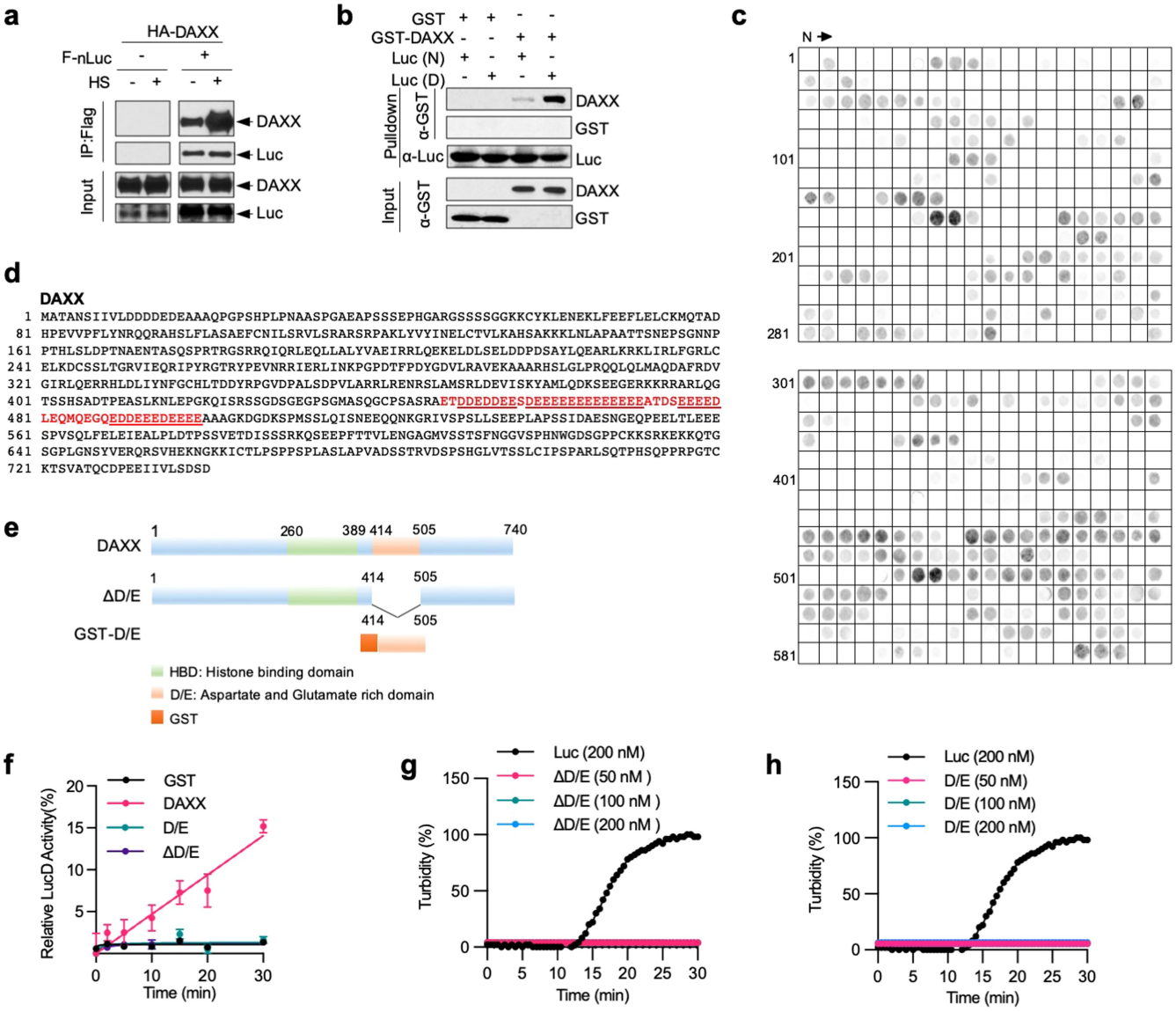

Extended Data Fig. 5 | DAXX binds to misfolded proteins and depends on the polyD/E region for its activity. a, The DAXX-luciferase interaction is increased upon heat shock. HEK293T cells were transfected with HA–DAXX and Flag–nLuc as indicated, and treated with or without heat shock. Cell lysates were immunoprecipitated with anti-Flag mAb (M2) beads. Input and immunoprecipitated samples were analysed by western blot. **b**, DAXX preferentially binds to heat-denatured luciferase. GST or GST–DAXX (100 nM each) was incubated with native (N) or heat-denatured (D) 6xHis-luciferase immobilized on Ni-NTA agarose. The input and pulldown samples were analysed by western blot. **c**, Binding of DAXX to cellulose-bound peptide scans derived from luciferase, p53, MDM2, H3.3, H4 and DAXX. Each peptide contained thirteen amino acid residues that overlapped adjacent peptides by ten. **d**, Protein sequence of DAXX. The poly D/E region is marked in red colour, and the four continuous runs of Asp/Glu (with 14, 11, 7, and 5 residues, respectively) are underlined. **e**, Schematic presentation of full-length DAXX and its mutants. DAXX(D/E) was fused to GST at the N terminus for protein stabilization. **f**, DAXX(ΔD/E) and DAXX(D/E) lack unfoldase activity. Misfolded LucD monomers (50 nM) were incubated with DAXX(ΔD/E) or DAXX(D/) (100 nM each) for the indicated times and assayed for luciferase activity (,ean ± s.d., $n = 3$). **g**, **h**, DAXX(ΔD/E) and DAXX(D/E) remain soluble during heat treatment. Recombinant DAXX ΔD/E (**g**) and D/E (**h**) proteins were heated at 42 °C for the indicated durations. Luciferase (200 nM) was used as a positive control. Aggregation formation was monitored by OD_{600} and normalized to the luciferase control. Assays in **a**–**c** have been performed two times with similar results. Numerical data are mean or mean ± s.d. ($n = 3$) and are representative of two independent experiments (**f**–**h**).

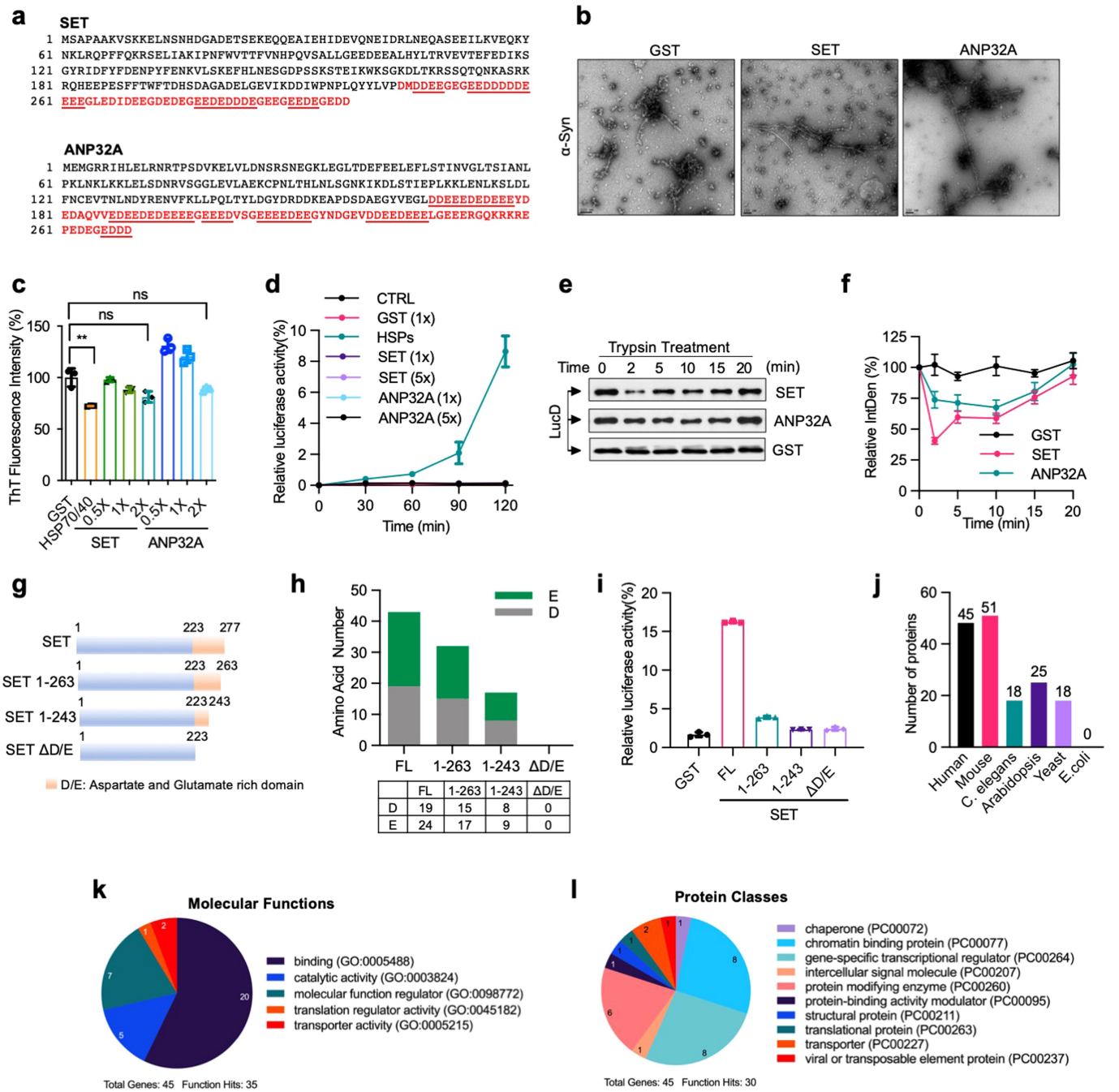

	FL	1-263	1-243	ΔD/E
D	19	15	8	0
E	24	17	9	0

Extended Data Fig. 6 | Role of other polyD/E proteins in protein folding. **a**, Sequences of human SET and ANP32A proteins. The poly D/E region is marked in red colour, and the continuous runs of Asp/Glu are underlined. **b**, **c**, ANP32A and SET does not block α-Syn fibrillization. α-Syn monomers (70 μM) were incubated with SET or ANP32A (0.4 μM each) for 7 days. Samples were analysed by electron microscopy (**b**) and ThT staining (**c**). Scale bar, 100 nm. **d**, SET and ANP32A are unable to solubilize urea-denatured luciferase. Urea-denatured luciferase (5 nM) was incubated with GST, SET, ANP32A (0.2 μM each) or HSPs (0.2 μM HSP70, 0.1 μM HSP40, and 0.4 μM HSP104(A503S)) at 25 °C for 90 min. Activity relative to that of the native control are shown. **e**, **f**, Unfoldase activity of ANP32A and SET. Misfolded LucD (50 nM) was incubated with GST, SET or ANP32A (200 nM each) at 25 °C. At indicated time points, aliquots of refolding luciferase were incubated with 2.5 μM trypsin at 22 °C for 2 min, denatured in SDS sample buffer, and analysed by western blot (**e**), with the quantification showed in (**f**). **g**, **h**, Schematic presentation of SET and its deletion mutants (**g**), and the numbers of Asp (D) and Glu (E) in each mutant (**h**). **i**, Heat-inactivated luciferase (5 nM) was incubated at 25 °C with SET or its deletion mutants (200 nM each) for 90 min. Activity relative to that of native luciferase are shown. **j**, Number of polyD/E proteins different species. **k**, **l**, Gene Ontology analysis of polyD/E proteins in humans. Proteins are classified into pie chart based on their molecular functions (**k**) and protein classes (**l**). Assays have been performed two (**b**) or three (**e**) times with similar results. Numerical data are mean ± s.d. ($n = 3$) and are representative of two independent experiments (**c**, **d**, **f**, **i**). **$P < 0.01$, unpaired Student's t-test.

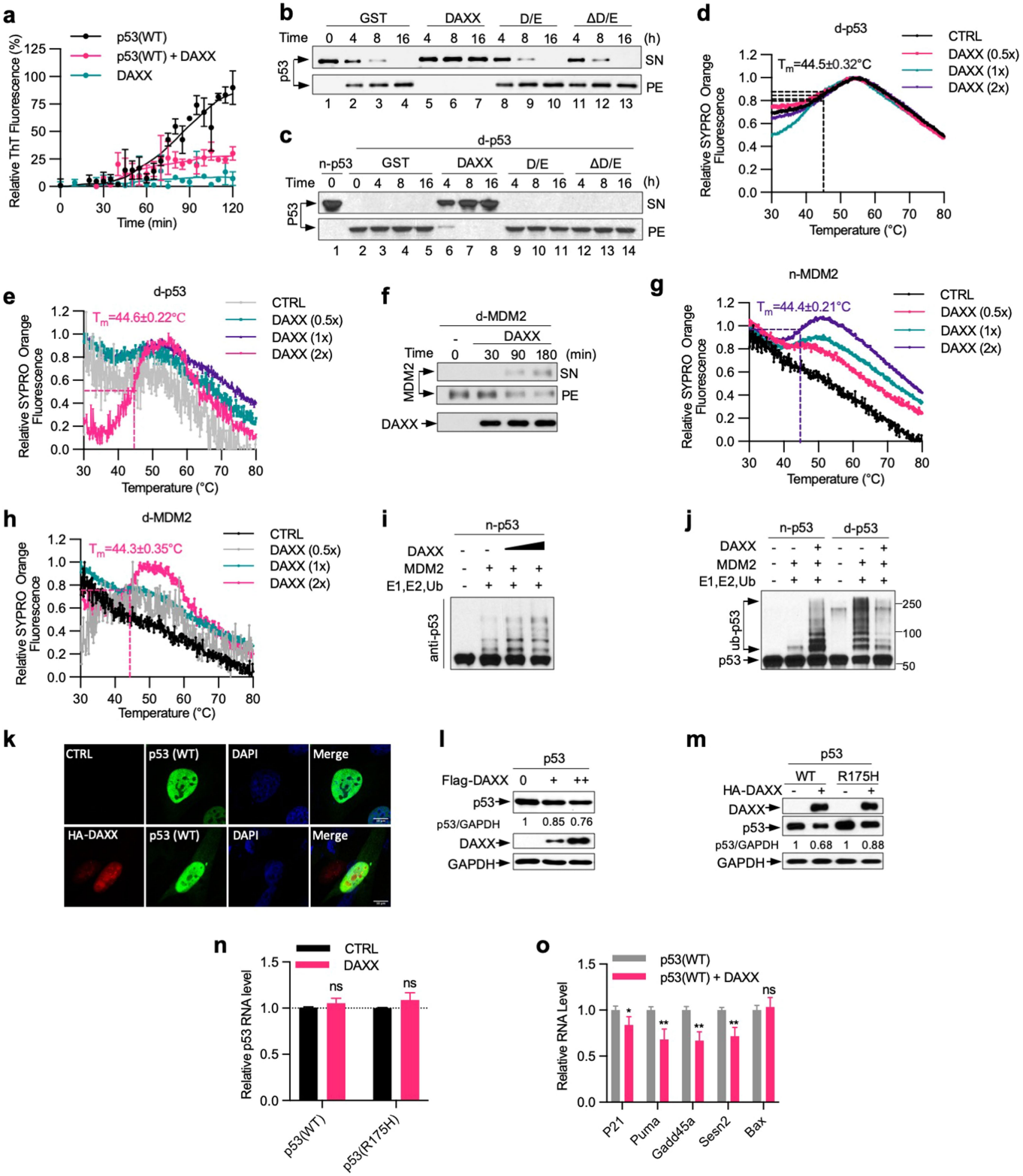

Extended Data Fig. 7 | See next page for caption.

Extended Data Fig. 7 | DAXX maintains the native conformation of both p53 and MDM2. a, DAXX abrogates p53 fibrillization. Recombinant wild-type p53 and DAXX–6xHis proteins (5 μM each) were incubated alone or together at 37 °C for 2 h in the presence of ThT (25 μM). Formation of amyloid fibrils was assayed by ThT. **b**, **c**, DAXX(ΔD/E) and DAXX(D/E) cannot protect p53 from aggregation. Native p53 (n-p53) (**b**), or denatured p53 aggregates (d-p53) (**c**), (100 nM each) was incubated with GST, Flag–DAXX, DAXX(D/E) or DAXX(ΔD/E) (200 nM each) at 37 °C (**b**) or at 25 °C (**c**) for the indicated times. Samples were partitioned into supernatant (soluble) and pellet (insoluble) fractions via sedimentation, and analysed by western blot. As in Fig. 4a, b except that DAXX(D/E) and DAXX(ΔD/E) samples are included. **d**, **e**, **g**, **h**, DAXX restore native conformation to denatured p53 and MDM2. Native p53 (**d**) or native MDM2 (n-MDM2, **g**), or denatured p53 (**e**) or MDM2 (d-MDM2, **h**), (1 μM each) was incubated alone or together with GST or DAXX–6xHis (0.5, 1, 2 μM, from Sf9 cells) at the indicated molar ratios for 3 h and analysed by thermal shift assay. The transition of the unfolding curve represents the temperature at which the protein unfolding occurs (T_m). **f**, DAXX dissolve preformed MDM2 aggregates. d-MDM2 (100 nM) was incubated with Flag–DAXX (200 nM) at 25 °C for the indicated times. Supernatant (soluble) and pellet (insoluble) fractions after sedimentation were analysed by western blot. **i**, DAXX enhances MDM2-mediated p53 ubiquitination. Native p53 (20 nM) was incubated with native MDM2 (45 nM) in the presence or absence of DAXX (20 or 100 nM) at 37 °C for 1.5 h. E1, E2 and His-ubiquitin (His-Ub) were then added for in vitro ubiquitination assay. The reaction mixtures were analysed by western blot. **j**, Native MDM2-mediated ubiquitination of native p53 (20 nM) in the presence or absence of Flag–DAXX (100 nM), or of denatured p53 (20 nM) pre-incubated with or without Flag–DAXX (100 nM) for 3 h at 25 °C. **k**, **l**, DAXX reduces p53 levels in cells, but does not alter the largely diffuse nuclear localization pattern of p53. Flag–p53 was transfected into U2OS cells together with empty vector or DAXX. Cells were analysed by immunofluorescence (**k**) and western blot (**l**). **m**–**o**, H1299 cells inducibly expressing wild-type p53 or p53(R175H) were transfected with control vector (–) or HA–DAXX. Upon induction of p53 expression by Dox (1 μg ml^{-1}), cells were analysed for protein levels by western blot with relative p53/GAPDH ratios indicated (**m**) and for mRNA levels of *p53* (**n**) and p53 target genes (**o**) by qRT–PCR. Scale bar, 10 μm. Assays in panels have been performed two (**d**, **e**, **g**, **h**, **k**–**m**) or three (**b**, **c**, **f**, **i**, **j**) times with similar results. Numerical data are mean ± s.d. ($n = 3$) and are representative of two independent experiments (**a**, **n**, **o**). *$P < 0.05$, **$P < 0.01$, ns, not significant; unpaired Student's *t*-test.

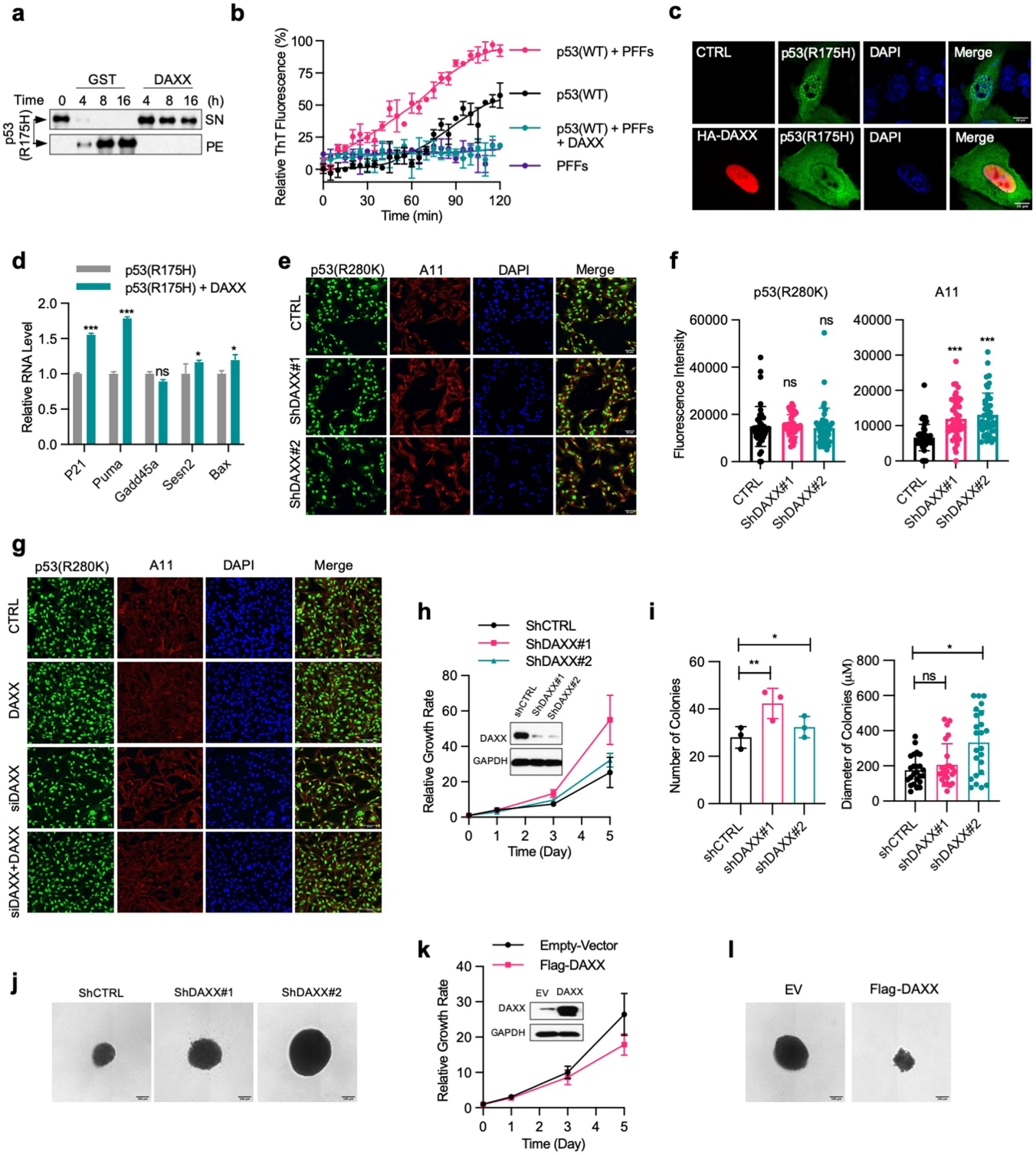

Extended Data Fig. 8 | See next page for caption.

Extended Data Fig. 8 | DAXX restores native conformation and function of mutant p53. a, DAXX prevents p53(R175H) aggregation. p53(R175H) protein (100 nM) was incubated with GST or Flag–DAXX (200 nM each) at 37 °C for the indicated times. SN and pellet fractions were analysed by western blot. **b**, DAXX blocks p53(R175H) PFF-induced fibrillization of p53. Wild-type p53 (5 μM) was incubated with or without p53(R175H) PFFs and DAXX as indicated. Fibril formation was assayed by ThT binding. **c**, DAXX reduces p53(R175H) aggregates in cells. Flag–p53(R175H) was transfected into the U2OS cells together with empty vector (Ctrl) or HA–DAXX. Cells were analysed by immunofluorescence. Scale bar, 10 μm. Part of the images are also shown in Fig. 4i. **d**, DAXX partially restores the function of mutant p53. H1299 cells inducibly expressing p53(R175H) were transfected with control vector (–) or HA–DAXX. Upon induction of p53 expression by Dox (1 μg ml^{-1}), cells were analysed for the expression of p53 target genes by RT–PCR. **e**–**g**, Effect of DAXX on aggregation of endogenous mutant p53. MDA-MB-231 cells were transduced with lentiviral vectors expressing control or DAXX shRNA (**e**, **f**), or transfected with control siRNA, *DAXX* siRNA, and/or an siRNA-resistant form of DAXX (Flag–DAXX) as indicated (**g**). Cells were immunostained with anti-p53 (DO-1) and anti-fibrillar oligomer (A11) antibodies (**e**, **g**) and quantified (**f**). Scale bar, 50 μm. **h**-**j**, Knocking down DAXX enhances growth and tumorigenicity of MDA-MB-231 cells. Control and DAXX-knockdown MDA-MB-231 cells were assayed for adherent proliferation, protein expression (**h**), and soft-agar colony formation (21 days), with number and sizes of colonies (**i**) and representative images of colonies (**j**) shown. **k**, **l**, Overexpressing DAXX inhibits growth and tumorigenicity of MDA-MB-231 cells. MDA-MB-231 transduced with pBabe or pBabe-Flag-DAXX were assay for adherent proliferation for 5 days (**k**) and soft-agar colony formation (21 days), with representative images of colonies shown (**l**). Assays have been performed two (**a**) or three (**c**, **e**, **g**) times with similar results. Numerical data are mean ± s.d. ($n = 3$ for **b**, **d**, and 6 for **i**, **h**, **k**) and are representative of three independent experiments. $^{*}P < 0.05$, $^{**}P < 0.01$, $^{***}P < 0.001$; unpaired Student's *t*-test.

Extended Data Table 1 | Human polyD/E proteins containing 35 or more D or E residues in any 50-residue window

UniProt ID	Symbol	Protein Name	D	E	D/E Position	D/E sequence	Molecular Function (GO)
Q86V15	CASZ1	Zinc finger protein castor homolog 1	19	16	1680-1730	EELELPEEEAEDDEDEDDDEDDDEDDDEDDDEDLRTDSEESLPEAAAE	Transcription factor
P37275	ZEB1	Zinc finger E-box-binding homeobox 1	4	31	1031-1081	EEDEDSEKEEEEEDKEMEELQEEKECEKPQGDEEEEEEEEEVEEEEVEEA	KRAB box transcription factor
Q9UFB7	ZBTB47	Zinc finger and BTB domain-containing protein 47	1	34	285-335	EEEEEEEEEEGGGSGREEEEEEGGSQGEEEEEEEDGHSEQEEEEEEEEE	KRAB box transcription factor
Q01538	MYT1	Myelin transcription factor 1	2	33	274-324	DEEEEEEEEEEEEEEEEEEEEEEEEEEEEEAAPDVIFQEDTSHTSAQ	zinc finger transcription factor
Q9UL68	MYT1L	Myelin transcription factor 1-like protein	8	27	131-181	EEEEIEEEDEDDDEDGEDVEDEEEEEEEEEEEEEEEEDHQMNCHNTRI	zinc finger transcription factor
Q7Z6M4	MTERF4	Transcription termination factor 4, mitochondrial	26	13	330-380	STSDDKRASLDEDEDDDDEEDNDEDDNDEDDDDEDDDEAEDNDEDEDDDE	Transcription termination factor
Q4LE39	ARID4B	AT-rich interactive domain-containing protein 4B	9	26	520-570	AEEEKAKSGDETNKEEDEDDEEAEEEEEEEEEEEDEDDDDNNEEEEFECY	Transcription cofactor
O60841	EIF5B	Eukaryotic translation initiation factor 5B	5	30	525-575	IEVKENPEEEEEEEEEEEEDEESEEEEEEGESEGSEGDEEDEKVSDEKD	Translation initiation factor
O60721	SLC24A1	Sodium/potassium/calcium exchanger 1	3	32	854-904	SDGGDSEEEEEEEEQEEEEEEEQEEEEEEEEEEEKGNEEPLSLDWPE	Transporter
Q12830	BPTF	Nucleosome-remodeling factor subunit BPTF	17	18	137-187	EEDMVSEEEEEDGDAEETQDSEDDEEDEMEEDDDDSDYPEEMEDDDDDA	Nucleosome-remodeling factor
Q15911	ZFHX3	Zinc finger homeobox protein 3	3	32	460-510	EEEAEEEEEEEEAEEEEEEEEEEEEEEEDEGCKGLFPSELDEELEDRPHE	DNA binding
P19338	NCL	Nucleolin	16	19	238-288	EEEDDEDEDDDDDEDDEDDDDEDDEEEEEEEEEEPVKEAPGKRKKEMAKQ	mRNA splicing
Q96MU7	YTHDC1	YTH domain-containing protein 1	7	28	222-272	DEEVDEDGEEEEEEEEEEEEEEEEEEEYEQDERDQKEEGNDYDTRSEAS	mRNA splicing
P0DME0	SETSIP	Protein SETSIP	19	20	251-301	EEGGEDDDDDDDDGDEGEEELEDIDEGDEDEGEEDEDDDEGEEGEEDEGE	Chaperone
Q01105	SET	Protein SET	16	24	239-629	DDEEGEGEEDDDDDEEEEGLEDIDEEGDEDEGEEDEDDDEGEEGEEDEGE	Chaperone
P27797	CLAR	Calreticulin	12	23	361-411	QDEEQRLKEEEEDKKRKEEEEAEDKEDDEDKDEDEEDEEDKEEDEEEDVP	Calcium-binding protein
P21817	RYR1	Ryanodine receptor 1	4	31	1876-1926	EEEDEEEEGEEEDEEEKEEDEEETAQEKEDEEKEEEEAAEGEKEEGLEEG	Ligand-gated ion channel
P0C7V8	DCAF8L2	DDB1- and CUL4-associated factor 8-like protein 2	1	34	97-147	GESLFHYPLVGEEETEREEDEEIQEEGGEEEEEEEEEEEEEEEEEEE	G-protein
P46060	RANGAP1	Ran GTPase-activating protein 1	2	33	361-411	EDEEEEEEGEEEEEEAEEEEEDEEEEEEEEEEEEEEPQQRGQGEKSATP	G-protein modulator
Q6PL18	ATAD2	ATPase family AAA domain-containing protein 2	23	12	251-301	QEHEDDGEDEDDDEDDDDDDDDDDDDDEDDEDEEDGEEENQKRYYLRQRK	Hydrolase
O43847	NRDC	Nardilysin	17	18	151-201	EEEEDDDEDSGAEIEDDDEEGFDDEDEFDDEHDDDLDTEDNELEELEERA	Metalloprotease
Q7Z6Z7	HUWE1	E3 ubiquitin-protein ligase HUWE1	17	18	2427-2477	DEDDSQDEEEEEEEDEEDDQEDDEGEEGDEDDDDDGSEMELDEDYPDMNA	Ubiquitin-protein ligase
Q8WYB5	KAT6B	Histone acetyltransferase KAT6B	2	33	1069-1119	SEEEEEEEDEEEEEEEEEEEEEDEEEEEEEEEEEEEENIQSSPPRLTKPQS	Acetyltransferase
O15355	PPM1G	Protein phosphatase 1G	8	27	264-314	SDEAEEEEEDSEECSEEEDGYSSEEAENEEDEDDTEEAEEDDEEEEEEMM	Protein serine/threonine phosphatase
Q5TCY1	TTBK1	Tau-tubulin kinase 1	2	33	737-787	EEEEDEEEEEEDEEEEEEEEEEEEEEEEEEEEEEAAAAVALGEVLGPRS	Non-receptor serine/threonine protein kinase
Q92688	ANP32B	Acidic leucine-rich nuclear phosphoprotein 32 family member B	13	22	193-243	EDDEDEDVEGDEDDDEVSEEEEEFGLDEEDEDEDEDEEEEEGGKGEKRKR	Phosphatase inhibitor
P39687	ANP32A	Acidic leucine-rich nuclear phosphoprotein 32 family member A	9	26	186-236	VEDEEDEDEEEEGEEEDVSGEEEEDEEGYNDGEVDDEEDEEELGEEERGQ	Phosphatase inhibitor
Q9BTT0	ANP32E	Acidic leucine-rich nuclear phosphoprotein 32 family member E	7	28	167-217	DEDDEEEEEENEAGPPEGYEEEEEEEEEEDEDEDEDEDEAGSELGEGEEEV	Phosphatase inhibitor
P17480	UBTF	Nucleolar transcription factor 1	19	16	694-744	EEDDENGDSSEDGGDSSESSSEDESEDGDENEEDDEDEDDDEDDDEDEDN	Others
Q69YN4	VIRMA	Protein virilizer homolog	13	22	250-300	EDEDDVDVEEEEDEDEDDRRTVDSIPEEEEEDEEEEGEEDEEGEGDDGYE	Others
Q9UER7	DAXX	Death domain-associated protein	8	27	443-493	SDEEEEEEEEEEEEEATDSEEEEDLEQMQEGQEDDEEEDEEEEEAAAGKDG	Others
Q9Y4B6	DCAF1	DDB1- and CUL4-associated factor 1	17	18	1396-1446	EDEDEEEDQEEEDQEEDDDDEDDDDTDDLDELDTDQLLEAELEEDDNNEN	Others
Q8TC90	CCER1	Coiled-coil domain-containing glutamate-rich protein 1	2	33	307-357	VEDEEEEVEDEEEEEVEEAEYVEEGEEELEEEELEEEEVLEENEQRGEE	Others
Q6ZU64	CFAP65	Cilia- and flagella-associated protein 65	1	34	1760-1810	KEEGEEEKGEEEEEELEEEEEEEEETEEEELGKEEIEEKEEERDEKEEKV	Others
P07199	CENPB	Major centromere autoantigen B	4	31	422-472	GEEEEEEGEEEEEEGGEGEELGEEEVEEEGDVDSDEEEEEDEESSSEGL	Others
Q9UIF8	BAZ2B	Bromodomain adjacent to zinc finger domain protein 2B	18	17	610-660	DEEEDDEEEDEEDDEDDESDDSQSESDSNSESDTEGSEEEDDDDKDQDES	Others
Q9HAW4	CLSPN	Claspin	2	33	629-679	EEEEEEEEEMTDESEEDGEEKVEKEEKEEELEEEEKEEEEEEGNQETA	Others
Q8IZL8	PELP1	Proline-, glutamic acid- and leucine-rich protein 1	2	33	925-975	EEEEEEFEEEFEEEEGELEEEEEEEDEEEEEELEEVEDLEFGTAGGEVEE	Others
P20962	PTMS	Parathymosin	6	29	38-88	VEEEENGAEEEEEETAEDGEEEDEGEEEDEEEEEEEDDEGPALKRAAEEED	Others
Q12899	TRIM26	Tripartite motif-containing protein 26	7	28	386-436	GDEEEEGEEEEEEEEAGYGDGYDDWETDEDEESLGDEEEEEEEEEEEVLE	Others
A1YPR0	ZBTB7C	Zinc finger and BTB domain-containing protein 7C	20	15	137-187	DDKEDDDDDEDDDDEEDEEEEEEEEEDDDDDTEDFADQENLPDPQDISCH	Others
Q7L0X2	ERICH6	Glutamate-rich protein 6	0	35	26-76	EEEEEEEEVEEEEEEVEEEEEEVEEEEEEVVEEELVGEEQELEAPETFSE	Others
Q86TY3	ARMH4	Armadillo-like helical domain-containing protein 4	14	21	604-654	LDQLESEEGQEDEDEEDEEDEDEEEEDEEEDEEDKDADSLDEGLDGDTEL	Others
Q8IZU1	FAM9A	Protein FAM9A	0	35	227-277	KEEEEEKEEEEEEGEEEGGGEEGEEGGGGGEGEETEEEEEEEEEEEEEQ	Others
A0A0A0MQV9	SETD18	Histone-lysine N-methyltransferase	15	20	1049-1099	EEEEEAEEEEEEDDDDDSDDRDESENDDEDTALSEASEKDEGDSDEEE	Others

PolyD/E-containing proteins from human are listed with UniProt IDs (1st column), protein symbols (2nd column), and protein names (3rd column) indicated. The numbers of D and E residues within the region are listed in the 4th and 5th columns,respectively. Sequences of poly D/E region are listed in the 6th column with D/E marked in red. GO terms are listed in the last column. All proteins are clustered into different categories depending on the protein class or molecular function (Extended Data Fig. 6k, l).

nature research

Corresponding author(s): Dr. Xiaolu Yang

Last updated by author(s): Jun 27, 2021

Reporting Summary

Nature Research wishes to improve the reproducibility of the work that we publish. This form provides structure for consistency and transparency in reporting. For further information on Nature Research policies, see Authors & Referees and the Editorial Policy Checklist.

Statistics

For all statistical analyses, confirm that the following items are present in the figure legend, table legend, main text, or Methods section.

n/a	Confirmed	
☐	☒	The exact sample size (*n*) for each experimental group/condition, given as a discrete number and unit of measurement
☐	☒	A statement on whether measurements were taken from distinct samples or whether the same sample was measured repeatedly
☐	☒	The statistical test(s) used AND whether they are one- or two-sided *Only common tests should be described solely by name; describe more complex techniques in the Methods section.*
☒	☐	A description of all covariates tested
☐	☒	A description of any assumptions or corrections, such as tests of normality and adjustment for multiple comparisons
☐	☒	A full description of the statistical parameters including central tendency (e.g. means) or other basic estimates (e.g. regression coefficient) AND variation (e.g. standard deviation) or associated estimates of uncertainty (e.g. confidence intervals)
☐	☒	For null hypothesis testing, the test statistic (e.g. *F*, *t*, *r*) with confidence intervals, effect sizes, degrees of freedom and *P* value noted *Give P values as exact values whenever suitable.*
☒	☐	For Bayesian analysis, information on the choice of priors and Markov chain Monte Carlo settings
☒	☐	For hierarchical and complex designs, identification of the appropriate level for tests and full reporting of outcomes
☒	☐	Estimates of effect sizes (e.g. Cohen's *d*, Pearson's *r*), indicating how they were calculated

Our web collection on statistics for biologists contains articles on many of the points above.

Software and code

Policy information about availability of computer code

Data collection	Zeiss Zen 2.3 was used to acquire images. Bio-Rad NGC Chromatography System was used to collect chromatography data and BioTek Gen 5 was used to collect microplate reader data.
Data analysis	Fiji (Image J 1.52p) was used to contrast and overlay images. Prism 8 was used for all statistical analyses and graph plotting. Asp and Glu enrichment analysis was performed with code available at https://github.com/SunmoonTao/de-enrichemnt-analysis by Python Note (3.7.10) and Excel (version 16.5). Jupyter notebook 5.7.8 Geneontology analysis was performed by website http://pantherdb.org

For manuscripts utilizing custom algorithms or software that are central to the research but not yet described in published literature, software must be made available to editors/reviewers. We strongly encourage code deposition in a community repository (e.g. GitHub). See the Nature Research guidelines for submitting code & software for further information.

Data

Policy information about availability of data

All manuscripts must include a data availability statement. This statement should provide the following information, where applicable:

- Accession codes, unique identifiers, or web links for publicly available datasets
- A list of figures that have associated raw data
- A description of any restrictions on data availability

Source code and datasets for polyD/E protein analysis are available in GitHub: https://github.com/SunmoonTao/de-enrichemnt-analysis. All other data supporting the findings of this study are provided within the manuscript and its Supplementary Information."

Field-specific reporting

Please select the one below that is the best fit for your research. If you are not sure, read the appropriate sections before making your selection.

☒ Life sciences ☐ Behavioural & social sciences ☐ Ecological, evolutionary & environmental sciences

For a reference copy of the document with all sections, see nature.com/documents/nr-reporting-summary-flat.pdf

Life sciences study design

All studies must disclose on these points even when the disclosure is negative.

Sample size	Sample size were not applicable.
Data exclusions	No data were excluded from the analysis.
Replication	Replicates are indicated in the Figure Legends or Methods. Luciferase activity assay, RT-QuIC assay, thermal shift assay, ThT binding assay and microscopy experiments were done in triplicate. Experiments involving Western Blotting (eg. In vitro unbiquitination, GST-Pull Down and sedimentation assay) were repeated independently at least twice and all attempts of replication gave similar results.
Randomization	The cells and sample region for imaging were evenly allocated and selected randomly. There was no requirement of randomization for other data.
Blinding	The core facility staffs who performing Electron Microscope imaging and Mass Spectrum were unaware of the sample identity. For all other experiments, investigators were not blinded to group allocation during data collection and analysis.

Reporting for specific materials, systems and methods

We require information from authors about some types of materials, experimental systems and methods used in many studies. Here, indicate whether each material, system or method listed is relevant to your study. If you are not sure if a list item applies to your research, read the appropriate section before selecting a response.

Materials & experimental systems

n/a	Involved in the study
☐	☒ Antibodies
☐	☒ Eukaryotic cell lines
☒	☐ Palaeontology
☒	☐ Animals and other organisms
☒	☐ Human research participants
☒	☐ Clinical data

Methods

n/a	Involved in the study
☒	☐ ChIP-seq
☒	☐ Flow cytometry
☒	☐ MRI-based neuroimaging

Antibodies

Antibodies used	Antibodies against the following proteins/epitopes were purchased from the indicated sources: GAPDH (sc-47724,Mouse, WB, IP, IF and IHC(P)), His (sc-8036, Mouse, IP, WB, IHC(P), ELISA, IF, FCM), GST (sc-138, Mouse, IP, WB, IHC(P), ELISA, IF, FCM), p53-DO1 (sc-126, Mouse, WB, IP, IF, IHC(P) and FCM), Mdm2 (sc-965, Mouse, WB, IP, IF and IHC(P)), DAXX (sc-8043, Mouse IP,WB, IHC(P), ELISA, IF, FCM), α-synuclein syn211 (sc-12767, Mouse, IP, WB, IHC(P), ELISA, IF, and FCM) (Santa Cruz Biotechnology); Flag (#14793, Rabbit, WB, IP, IHC, ChIP, IF, FCM, ELISA) and DAXX (#4533S, Rabbit, WB, IP, IHC, ChIP, IF, FCM, ELISA) (Cell Signaling Technology); p53 (PAb1620, #OP33, Mouse, WB, IP, IF; PAb240, #OP29, Mouse, WB, IP), and Mdm2 (#OP46, Mouse, WB, IP) (Calbiochem); and HA (ab137838, Rabbit, WB, ICC/IF, IP) and Luciferase (ab21176, Rabbit, ICC/IF, WB) (Abcam); β-Amyloid 1-42 (#805509) (BioLegend, Mouse, WB, IHC(P), ELISA). HRP-conjugated anti-rabbit IgG (#7074S) and anti-mouse IgG (#7076S) secondary antibodies were purchased from Cell Signaling Technology; IRDye® 800CW (926-32211, Goat anti Rabbit) and IRDye® 680RD (926-68070, Goat anti Mouse) secondary antibodies were purchased from Li-Cor.
Validation	All the primary antibodies we used were commercial ones, and validated by manufacturers, please see manufacturer's website for details.

Eukaryotic cell lines

Policy information about cell lines

Cell line source(s)	293T cells (human, ATCC-CRL 3216) H1299 (human, ATCC-CRL 5803)

	U20S (human, ATCC-HTB 96) MDA-MB-231 (human, ATCC-HTB 26) SH-SY5Y (human, ATCC-CRL 2266) Sf9 (Spodoptera frugiperda, ATCC-CRL-1711)
Authentication	Cell lines are authenticated using STR profiling by DNA Sequencing Facility, Penn Medicine, University of Pennsylvania.
Mycoplasma contamination	Cell lines were tested for mycoplasma contamination and no indication of contamination was observed.
Commonly misidentified lines (See ICLAC register)	No commonly misidentified cell lines were used.